CHAPTER 9

ORE MINERAL ASSEMBLAGES OCCURRING IN IGNEOUS ROCKS AND VEIN DEPOSITS

9.1 INTRODUCTION

Ore minerals are not uniformly distributed in the earth's crust but generally occur in associations that are characteristic in their mineralogy, textures, and relationships to specific rock types. The existence of these characteristic associations, each containing its own typical suite of ore minerals, considerably simplifies the task of the ore microscopist, because it permits him or her to anticipate the minerals that are likely to be encountered once the general association has been recognized. The grouping of ores into characteristic associations is, of course, a useful empirical rule of thumb but is not intended as a rigid scientific classification. Such an empirical division also has the advantage that no genetic models are implied, even though a similar mode of origin is likely. Indeed, these associations largely result from the formation of the ores under characteristically limited physico-chemical conditions, the nature of which may often be inferred from detailed study of the ores. Chapters 9 and 10 present brief discussions of the most commonly encountered ore mineral assemblages and their textures, with the ores categorized according to their most widely recognized types. These types represent rather broad generalizations, and there is no attempt to make the finer subdivisions presented by Cox and Singer (1986). The various sections are not intended as exhaustive discussions of ore petrology, but they do include the currently accepted theories on ore genesis, because the authors believe that an understanding of ore mineralogy and textures is enhanced by some knowledge of the ore-forming process. The sections included should prepare the student for most of the ore mineral assemblages encountered in an introductory course and in most ore samples that he or she might examine; however, it is

important to be ever watchful for the unexpected and unusual minerals. In the identification of minerals other than those included in Appendix 1, we recommend that students refer to encyclopedic works such as Ramdohr's *The Ore Minerals and Their Intergrowths*, Uytenbogaardt and Burke's *Tables for the Microscopic Identification of Ore Minerals*, Picot and Johan's *Atlas des Mineraux Metalliques*, and Ixer's *Atlas of Opaque and Ore Minerals in Their Associations*.

9.2 CHROMIUM ORES ASSOCIATED WITH MAFIC AND ULTRAMAFIC IGNEOUS ROCKS

Mineralogy

Major	Chromite (ideally $FeCr_2O_4$, although always containing significant MgO, Al_2O_3, Fe_2O_3)
Minor	Sulfides of nickel, copper, and iron (pentlandite, pyrrhotite, chalcopyrite, gersdorffite, bornite, valleriite)
Trace	Platinum group minerals (ferroplatinum, cooperite, laurite, stibiopalladinite, sperrylite, nickeliferous braggite), and rutile

Mode of Occurrence   There are two distinct modes of occurrence:

1. In layered basic intrusions as magmatic sediment layers
2. In peridotite or serpentinized peridotite masses associated with orogenic belts (sometimes termed "podiform" or "Alpine-type" chromites)

Examples   A classic example of a chromite deposit associated with a layered basic intrusion is the Bushveld Complex, South Africa; other examples include the Stillwater Complex, Montana (United States), and the Great Dyke (Rhodesia).

"Podiform" chromites occur in many orogenic belts and are generally much smaller deposits; important examples include deposits in Turkey, the Ural Mountains (Russia), the Philippines, and Cuba.

9.2.1 Mineral Associations and Textures

The few, isolated (although economically important) layered intrusions that can be regarded as chromium deposits occur in tectonically stable environments. The layers of the intrusive complexes can be regarded as magmatic "strata," which may be of considerable lateral extent. Within these, the chromite bands may range from a few millimeters to over 20 m in thickness and may show many features analogous to those shown in sedimentary rocks (lensing or wedging out, intraformational contortion, scour and fill structures). Pure chromite rocks (chromitites) may grade through various amounts of chromite + silicate (olivine, pyroxene) to normal dunites, peridotites, and so on. While commonly occurring in the olivine-rich layers, the chromite may

occur in significant amounts in any association that is *basic* in terms of overall composition. Although chromite itself is virtually the only ore mineral, it may show considerable differences in composition within deposits and between deposits of the "layered" and "podiform" types:

1. MgO/FeO ratios tend to be greater in podiform chromites (1–2.3) than in layered chromites (0.6–1).
2. Fe_2O_3 contents tend to be lower (<8 wt %) and Cr/Fe ratios higher (~1.5–4.5) in podiform chromites than in layered chromites (~10–24 wt % Fe_2O_3 and 0.75–1.75 Cr/Fe ratios, respectively).
3. Al_2O_3 and Cr_2O_3 have reciprocal relations (Cr_2O_3 being ~6.5–16 wt %, Al_2O_3 ~6–52 wt %) in podiform chromites and vary widely in layered chromites. The overall Al_2O_3/Cr_2O_3 ratio tends to be higher in podiform chromites.

In the layered intrusives, chromite commonly occurs as well-developed octahedral crystals (Figure 9.1), particularly when associated with larger amounts of interstitial material. In cases in which there is less interstitial material, the crystals develop polygonal interference boundaries (see Section 7.2).

The "podiform" or "Alpine-type" chromite ores occur in highly unstable tectonic environments, so that, in addition to the compositional differences
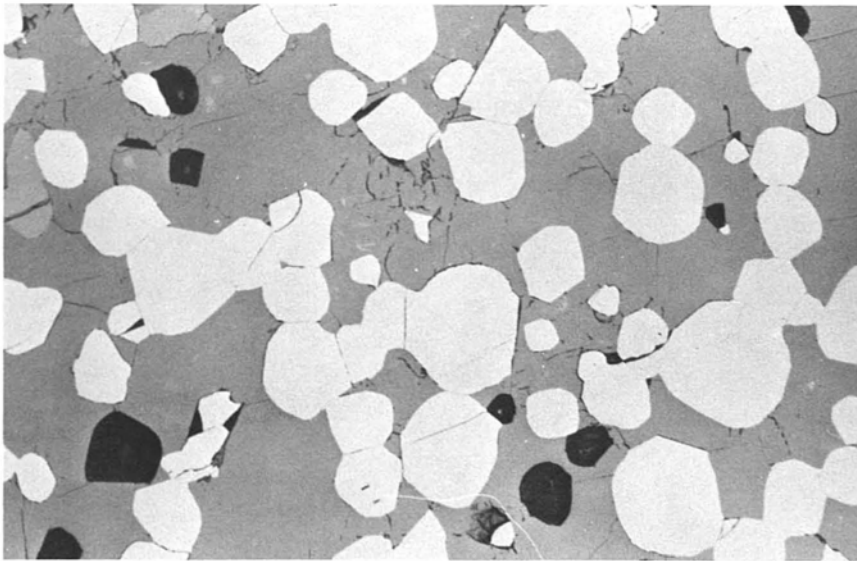

FIGURE 9.1   Euhedral grains of chromite (light gray) in a matrix of mafic silicate, Bushveld Complex, South Africa (width of field = 2,000 μm).

noted previously, there are marked textural differences. Although polygonal interference boundaries develop when there is very little interstitial material, the chromite grains are nearly always rounded when they are surrounded by silicate (Figure 9.2). These chromite grains can range from fine disseminations (<1.0 mm diameter) to the coarse textures (~1.5 cm diameter) of "leopard" or "grape" ore. Sometimes concentric shells of chromite and serpentine produce *orbicular* ores, and, in the chromites of both layered and podiform types, concentric compositional zoning may be developed, with outer zones exhibiting relative enrichment in iron (often observable under the microscope as a lighter peripheral zone). Such textures are often the result of hydrothermal alteration during serpentinization. Textures caused by deformation are also characteristic. Furthermore, the chromite grains and masses in podiform ores typically exhibit much fracturing in contrast to the undeformed grains of the layered chromites.

Both of the chromite associations just described may contain nickel concentrations of minor importance and concentrations of the platinum group metals that may be of considerable economic significance. Nickel in the layered intrusions occurs as sulfides and arsenides (assemblages of pyrrhotite-pentlandite-chalcopyrite with very minor gersdorffite, bornite, valleriite) in mafic horizons. These sulfide assemblages are similar to those discussed in Section 9.3 and are the result of a complex series of exsolution and inversion reactions. In the podiform chromites, most of the nickel occurs in solid solu-
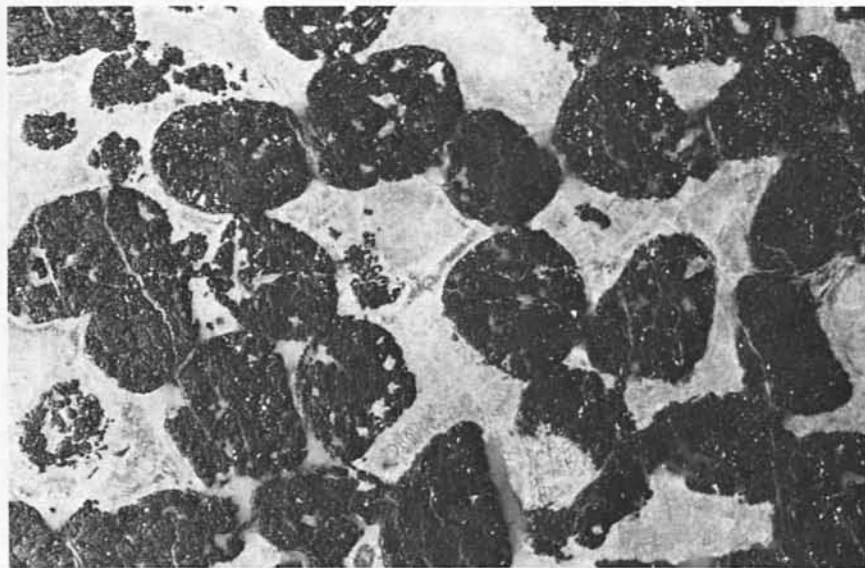

FIGURE 9.2 Rounded chromite aggregates in mafic silicate matrix, Greece. Note that, in the megascopic view, the chromite appears black, whereas, in the microscopic view in Figure 9.1, the chromite appears white (width of field = 3.5 cm).

tion in olivine and may be concentrated during weathering processes, although small amounts may occur as disseminated sulfides (pentlandite, heazlewoodite). The classic example of the concentration of platinum group metals in layered intrusives is the *Merensky "Reef,"* which is a persistent (~300 km) but thin (<1 m) layer of the Bushveld Complex. Between the top and bottom bounding chromite-rich bands of the so-called reef, the precious metal concentrations (as ferroplatinum, cooperite, laurite, stibiopalladinite, sperrylite, nickeliferous braggite, and native gold, Figure 9.3) reach a maximum and are associated with base metal sulfides of iron, nickel, and copper (pyrrhotite, pentlandite, chalcopyrite, valleriite).

9.2.2 Origin of the Ores

It is universally accepted that the chromite ores of layered intrusives are magmatic in origin and are related to processes of fractional crystallization and gravitative settling of layers of crystals on the floor of the intrusive sheets. The textures of the ores are wholly in accordance with such an origin. The major problems in the origin of these ore bodies are concerned with the mechanisms for producing essentially monomineralic chromite layers. Suggestions have included concentration by current sorting or preferential precipitation in response to changes in pressure, water content, oxygen fugacity or through multiple injections of magma. A mechanism proposed by Irvine (1974, 1977) is that of precipitation resulting from sudden extensive contamination of the parental basic magma with more acid liquid that has differentiated to a relatively siliceous composition. One mechanism, widely
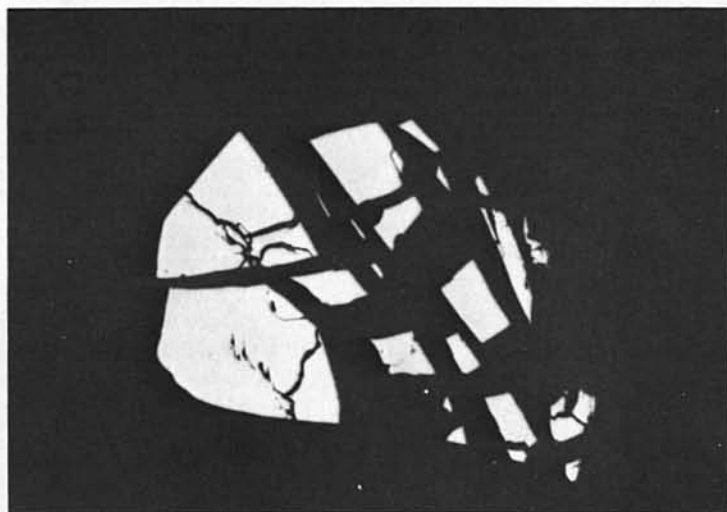

FIGURE 9.3 Fractured grain of sperrylite in a matrix of altered mafic silicates, Potgieterust, South Africa (width of field = 2,000 µm).

accepted as potential for platinum and chromite deposition, is that of a plume structure that rises into a magma chamber until it reaches a point of buoyancy, at which point it rapidly spreads laterally (Campbell, Naldrett, and Barnes, 1983). This would result in mixing and hence contamination over a wide area in a very short period of time. The addition of the silica-rich material in the contamination process forces the composition of the crystallizing melt (Figure 9.4) from the olivine + chromite cotectic curve (along which dis-seminated chromite admixed with olivine is forming) into the field of primary chromite crystallization (in which only chromite forms).

The origin of the podiform chromites is clearly very different, and it is closely related to the problem of the origin of the ultramafic rocks of Alpine type, which form part of so-called ophiolite complexes. Current theories relate the creation of ophiolites to processes along spreading boundaries between lithospheric plates. It has been suggested (see, e.g., Dickey, 1975; Lago, Rabinowicz, and Nicholas, 1982; Paktunc, 1990) that the podiform chromites
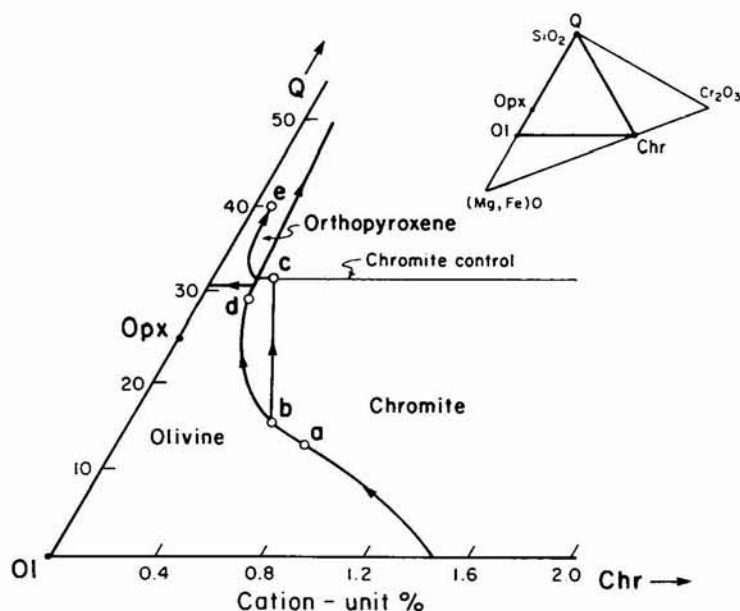

FIGURE 9.4   Projection of a portion of the SiO_2-Cr_2O_3-$(Mg,Fe)O$ system illustrating a possible mode of origin of chromite layers in stratiform intrusions. Coprecipitation of chromite and olivine from a magma beginning at point *a* would normally occur as the melt cooled along the cotectic *a-b-d* to *e* and would result in the formation of small and decreasing amounts of chromite. In contrast, if, after the melt had progressed from *a* to *b*, the melt were blended with another more silica-rich melt, the bulk composition of the liquid would shift into the primary crystallization field of chromite (point *c*). This would cause precipitation of only chromite, which would settle as a monomineralic layer, until the crystallizing liquid composirion returned to the chromite-olivine or chromite-orthopyroxene cotectic. (After Irvine, 1977; used with permission.)

form first as magmatic cumulates (much like the chromites of layered intrusives) in magma pockets or inclined cavities along these plate boundaries. Subsequent segregation with episodic mechanical disruption both during crystallization and in lateral transport away from the spreading zone results in "snowball" aggregation, rounding, and deformation of individual chromite blebs.

9.3 IRON-NICKEL-COPPER SULFIDE ORES ASSOCIATED WITH MAFIC AND ULTRAMAFIC IGNEOUS ROCKS

Mineralogy

Major	Pyrrhotite (both monoclinic and hexagonal varieties), pentlandite, pyrite, magnetite, chalcopyrite
Minor	Cubanite, mackinawite, platinum-group metal minerals, argentian pentlandite
Secondary	Millerite, violarite

Mode of Occurrence   Massive to disseminated in, or immediately associated with, mafic to ultramafic intrusive or extrusive rocks (gabbro, basalt, peridotite, norite) or metamorphosed mafic to ultramafic rocks.

Examples   Sudbury, Ontario; Thompson and Lynn Lake, Manitoba; Pechenga, Monchegorsk, and Noril'sk, Russia; Kambalda, W. Australia.

9.3.1 Mineral Associations and Textures

The iron-nickel-copper ores of this association occur as massive to disseminated sulfides (or sulfides plus oxides) in close association with mafic or ultramafic igneous rocks, notably norites and basalts. In most deposits of this type, pyrrhotite (commonly, in large part, the magnetic monoclinic variety) constitutes the principal ore mineral making up 80% or more of the ore. Chalcopyrite, the primary source of copper in these ores, is present as irregularly dispersed anhedral polycrystalline aggregates and veinlets. Pentlandite, the primary nickel- (and sometimes cobalt-) bearing phase, is usually not visible in rough hand specimens. It is, however, readily observed megascopically and microscopically in polished surfaces by its lighter color and higher reflectance relative to pyrrhotite. Under the microscope, Pentlandite is commonly observed in two distinct textures: (1) as granular polycrystalline veinlets (see Figures 9.5 and 8.8a); (2) as oriented lamellae and "flames" (see Figure 8.8b). The granular veinlets occur as irregular chain-like structures interstitial to pyrrhotite, chalcopyrite, and magnetite. The pentlandite, in addition to being slightly lighter in color than the pyrrhotite, is usually intensely fractured, a feature attributed to its having undergone a much greater volume reduction on cooling than the host pyrrhotite. The "flame" structure of pentlandite is one of the most diagnostic textures among ore minerals and results
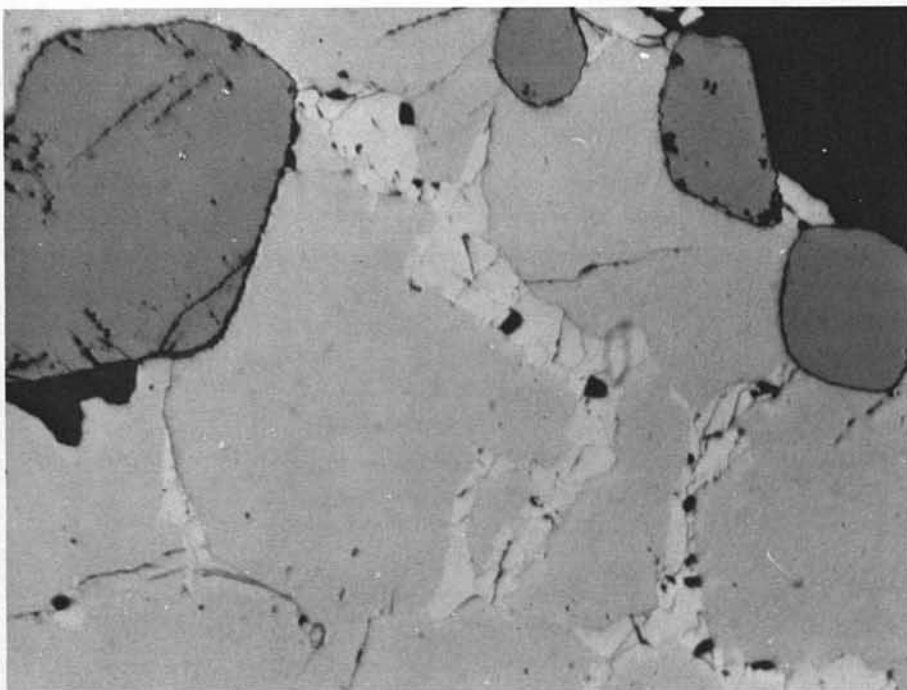
FIGURE 9.5   Fractured chain of pentlandite with pyrrhotite (lower side) and chalcopyrite (upper side) Clarabelle Mine, Sudbury, Ontario (width of field = 1,200 μm).

from crystallographically oriented exsolution of pentlandite from an originally formed nickel-bearing pyrrhotite.

Magnetite is present in these ores in rather variable quantities as euhedral, rounded, or even skeletal crystals dispersed within pyrrhotite (see Figure 9.5). The magnetite may be titaniferous and may contain oriented exsolution lamellae of ilmenite or ulvöspinel. Pyrite, although nearly always present, ranges from rare in the ores of the Sudbury District to a major constituent at Kambalda. Cubanite is generally present only in very minor proportions and nearly always as sharply defined laths within the chalcopyrite. The cubanite may be overlooked in a cursory examination because of its similarity to chalcopyrite, but it is readily noted under crossed polars due to its strong anisotropism. Mackinawite is common in small amounts as irregular grains and "worm-like" features within the chalcopyrite and is recognized by its strong anisotropism and bireflectance.

In addition to copper and nickel, these ores constitute major sources of the world's platinum group metals in the form of arsenides (sperrylite, $PtAs_2$), sulfarsenides (hollingworthite, $RhAsS$), bismuth- and antimony-bearing phases (froodite, $PdBi_2$), insizwaite, $PtBi_2$; sudburyite, $PdSb$), and tellurides (moncheite, $PtTe_2$; michenerite, $PdBiTe$), which may be present in trace quantities. These minerals are all characterized by high reflectances and occur as small

grains, which are rarely encountered in polished sections. Silver also occurs in some ores as solid solution in the pentlandite structure mineral argentian pentlandite [(Fe,Ni)$_8$AgS$_8$], and significant cobalt and gold are recovered from the ores.

9.3.2 Origin of the Ores

These iron-nickel-copper sulfide ores are generally considered to have formed as a result of the separation of an immiscible sulfide-oxide melt from a sulfur-saturated silicate melt shortly before, during, or after emplacement at temperatures of 900°C or above. The sulfide-oxide melt may have settled through the partly crystalline silicate magma or, if segregated early, may have been intruded separately; the resulting ores range from massive to disseminated, or even brecciated. When emplacement involves subaerial or submarine basaltic extrusions, the separated sulfides are commonly present as millimeter or smaller-sized rounded droplets dispersed within, or interstitial to, the silicates.

Studies of phase equilibria in the Cu-Fe-Ni-S and Fe-O-S systems reveal that the earliest formed sulfide phase, which may be accompanied by the formation of magnetite, is a nickeliferous and cupriferous pyrrhotite phase commonly referred to as the monosulfide solid solution (mss). The compositional limits of this phase at 600°C and above (Figure 9.6a) include the bulk compositions of many of the ores; hence, it appears that all or much of the entire sulfide mass formed initially as mss. During the subsequent cooling, as the compositional limits of the phase were considerably reduced (Figures 9.6b and 9.7), exsolution of chalcopyrite and then pentlandite or pyrite (depending on the bulk composition) occurred. The mss does not decompose entirely until temperatures of about 200°C are reached, and even then pentlandite exsolution from the remaining nickeliferous pyrrhotite apparently continues to temperatures as low as 100°C. The mineral paragenesis is summarized in Figure 8.9.

The early formed magnetite crystallized either as euhedral to subhedral or skeletal grains that appear to have changed very little except for internal exsolution of titanium as oriented blades of ilmenite or ulvöspinel. The major primary phase, the mss, has undergone considerable recrystallization and compositional change as copper and nickel have exsolved to form chalcopyrite and pentlandite, respectively. On cooling, the capability of the mss to retain copper is reduced to below 1% by 500°C; hence, most chalcopyrite (or its high-temperature analogue) formation occurs above this temperature. It remains as anhedral polycrystalline aggregates interstitial to the mss. Nickel, in contrast, may remain dissolved within the mss in very large amounts to temperatures below 200°C. The exsolution of the nickel in the form of pentlandite (which has a maximum thermal stability of 610°C) is controlled by the bulk composition of the mss (the compositions of most ores are such that pentlandite exsolves before pyrite). When temperature has decreased such that the composition of the ore no longer lies within the limits of the mss, pentlandite
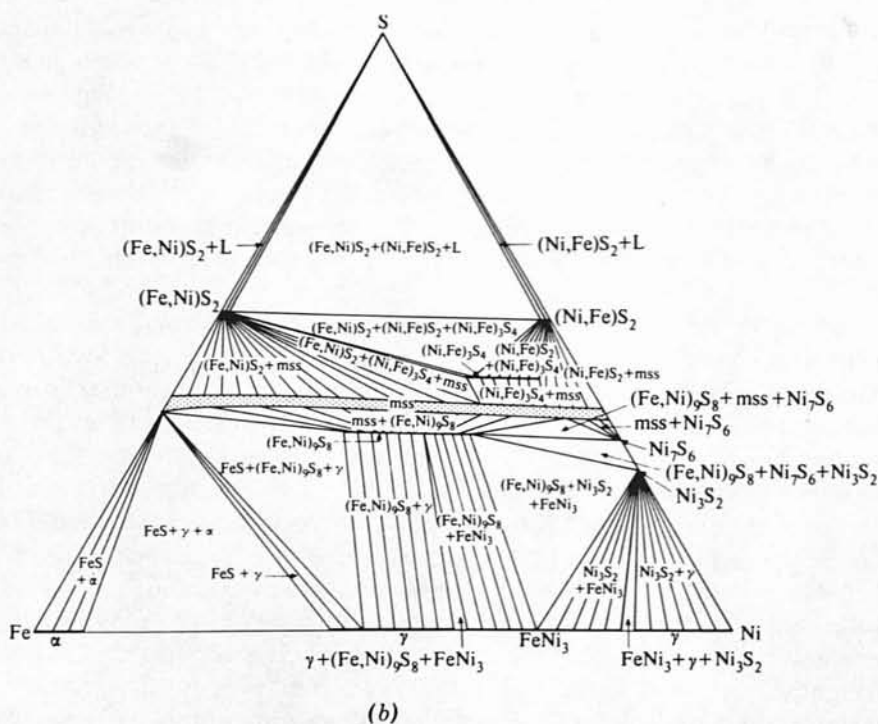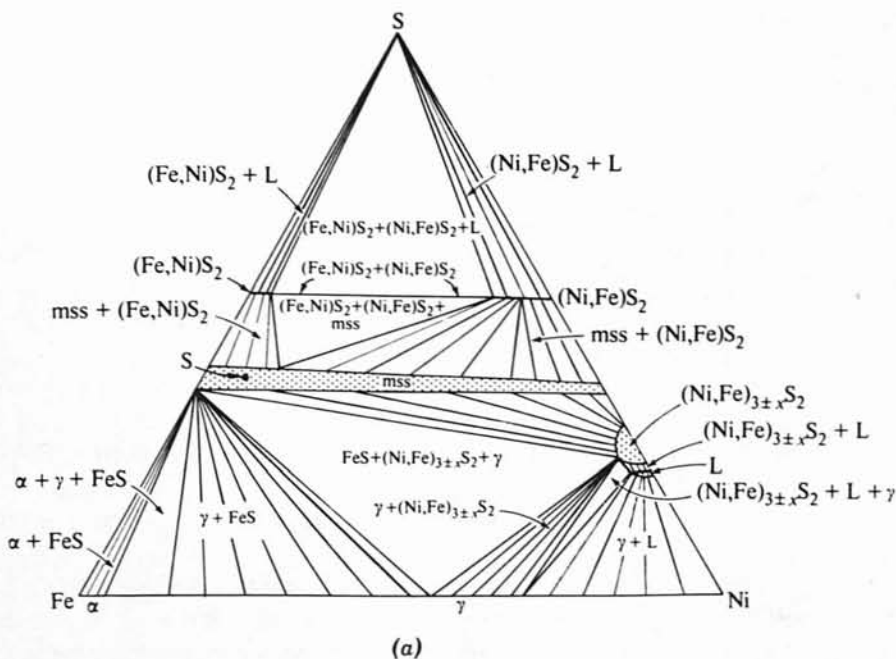
(a) diagram

S

(Fe,Ni)S$_2$ + L

(Ni,Fe)S$_2$ + L

(Fe,Ni)S$_2$+(Ni,Fe)S$_2$+L

(Fe,Ni)S$_2$

(Fe,Ni)S$_2$+(Ni,Fe)S$_2$

mss + (Fe,Ni)S$_2$

(Fe,Ni)S$_2$+(Ni,Fe)S$_2$+ mss

(Ni,Fe)S$_2$

mss + (Ni,Fe)S$_2$

S

mss

(Ni,Fe)$_{3\pm x}$S$_2$

(Ni,Fe)$_{3\pm x}$S$_2$ + L

FeS+(Ni,Fe)$_{3\pm x}$S$_2$+ γ

L

α + γ + FeS

(Ni,Fe)$_{3\pm x}$S$_2$ + L + γ

γ + FeS

γ+(Ni,Fe)$_{3\pm x}$S$_2$

α + FeS

γ + L

Fe α

γ

Ni

(a)

(b) diagram

S

(Fe,Ni)S$_2$+L

(Fe,Ni)S$_2$+(Ni,Fe)S$_2$+L

(Ni,Fe)S$_2$+L

(Fe,Ni)S$_2$

(Ni,Fe)S$_2$

(Fe,Ni)S$_2$+(Ni,Fe)S$_2$+(Ni,Fe)$_3$S$_4$

(Fe,Ni)S$_2$+(Ni,Fe)$_3$S$_4$+mss

(Ni,Fe)$_3$S$_4$ (Ni,Fe)S$_2$

(Fe,Ni)S$_2$+ mss

+(Ni,Fe)$_3$S$_4$

(Ni,Fe)$_3$S$_4$+(Ni,Fe)S$_2$+mss

(Ni,Fe)$_3$S$_4$+mss

mss

(Fe,Ni)$_9$S$_8$+ mss +Ni$_7$S$_6$

mss+ (Fe,Ni)$_9$S$_8$

mss+Ni$_7$S$_6$

(Fe,Ni)$_9$S$_8$

Ni$_7$S$_6$

FeS+(Fe,Ni)$_9$S$_8$+ γ

(Fe,Ni)$_9$S$_8$+Ni$_7$S$_6$+Ni$_3$S$_2$

(Fe,Ni)$_9$S$_8$+Ni$_3$S$_2$

Ni$_3$S$_2$

+FeNi$_3$

(Fe,Ni)$_9$S$_8$+ γ

FeS+ γ + α

(Fe,Ni)$_9$S$_8$

+FeNi$_3$

FeS
+ α

FeS + γ

Ni$_3$S$_2$
+FeNi$_3$

Ni$_3$S$_2$ Ni$_3$S$_2$+ γ

Fe α

γ

FeNi$_3$

γ Ni

γ+(Fe,Ni)$_9$S$_8$+FeNi$_3$

FeNi$_3$+ γ+Ni$_3$S$_2$

(b)

FIGURE 9.6   Phase relations in the condensed Fe-Ni-S system (a) at 650°C and (b) at 400°C. (From Vaughan and Craig, 1978; used with permission.)
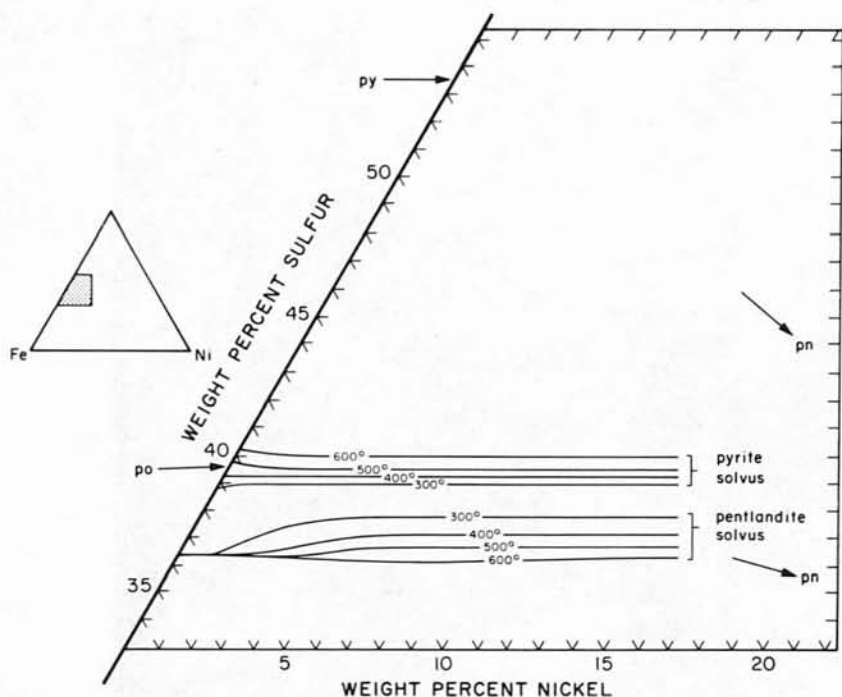
FIGURE 9.7 A portion of the Fe-Ni-S system showing the compositional limits of the monosulfide solid solution (mss) at 600°C, 500°C, 400°C, and 300°C. Pentlandite exsolves along the sulfur-poor boundary and pyrite along the sulfur-rich boundary.

begins to exsolve. If this occurs at a high enough temperature, diffusion rates are sufficiently rapid to permit segregation of the pentlandite into polycrystalline veinlets situated between the grains of mss (now becoming pyrrhotite). Diffusion of nickel from the mss to form crystallographically oriented exsolved pentlandite lamellae continues as the temperature decreases, but at ever-decreasing rates. Below 100–200°C, the diffusion rates are apparently insufficient for the exsolving pentlandite to migrate to grain boundaries of the mss, and the oriented lamellae known as "flames" are held within the mss as it finally expels most of the remaining nickel (natural pyrrhotites in these ores usually contain less than 0.5 wt % Ni). Whereas the early formed pentlandite probably grew at many points within the crystals, the last formed lamellae seem commonly to have formed along small fractures or other imperfections that provided the most favorable sites for nucleation.

9.3.3 Alteration Effects and Secondary Minerals

Surficial weathering of iron-nickel-copper ores characteristically leads to the formation of iron oxides and hydroxides along grain boundaries and fractures, the development of monoclinic pyrrhotite or even fine-grained porous pyrite along the boundaries of hexagonal pyrrhotite, and the replacement of
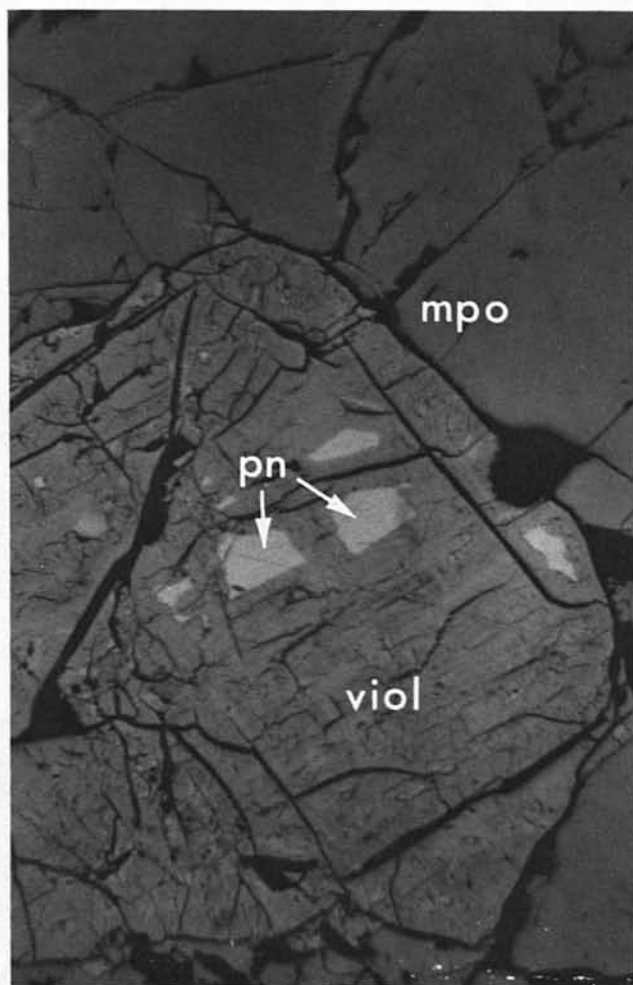
FIGURE 9.8 Violarite (viol) replacing pentlandite (pn) within unaltered monoclinic pyrrhotite (mpo), Lick Fork, Virginia (width of field = 40 μm). (Reproduced from J. R. Craig and J. B. Higgins, *Am. Mineral.* **60**, 36, 1975; used with permission.)

pentlandite by violarite, millerite, or both (see Figure 9.8). Secondary violarite is commonly porous and has a slight violet tint relative to the pyrrhotite; the millerite is distinctly yellow, accepts a fine polish, and is strongly aniso-tropic.

9.4 IRON-TITANIUM OXIDES ASSOCIATED WITH IGNEOUS ROCKS

Mineralogy
Major   Magnetite, ulvöspinel, ilmenite, rutile, hematite, apatite
Minor   Pyrite, chalcopyrite, maghemite, pyrrhotite
Secondary   Hematite, rutile, maghemite

Mode of Occurrence   Ores as thin layers to thick massive sheets or lenses in anorthositic, gabbroic, or noritic sequences in layered complexes and plutonic inrusives. Also common as accessory minerals in acid to basic igneous rocks.

Examples   Allard Lake, Quebec; Tahawus, New York; Duluth Gabbro, Minnesota; Bushveld Complex, S. Africa; Egersund, Norway.

9.4.1   Mineral Associations and Textures

Iron-titanium oxide ores are almost invariably composed of coarse (0.5–1.0 cm) equant grains of titaniferous-magnetite with or without ferrian ilmenite. Grains may be monomineralic, but exsolution lamellae of ulvöspinel oriented along the (100) or of ilmenite along the (111) (Figure 9.9) planes of the host magnetite are common. Such lamellae range from 0.1 mm across to submicroscopic in a "cloth-like" fabric. Hematite may be present as discrete grains but is most common as rims around, or lamellae within, magnetite or ilmenite. Magnetite and ilmenite, although similar at first glance, are readily distinguished by the faint pinkish to violet tint and anisotropism of the latter mineral. Ilmenite typically contains well-developed lamellar twinning (Figure
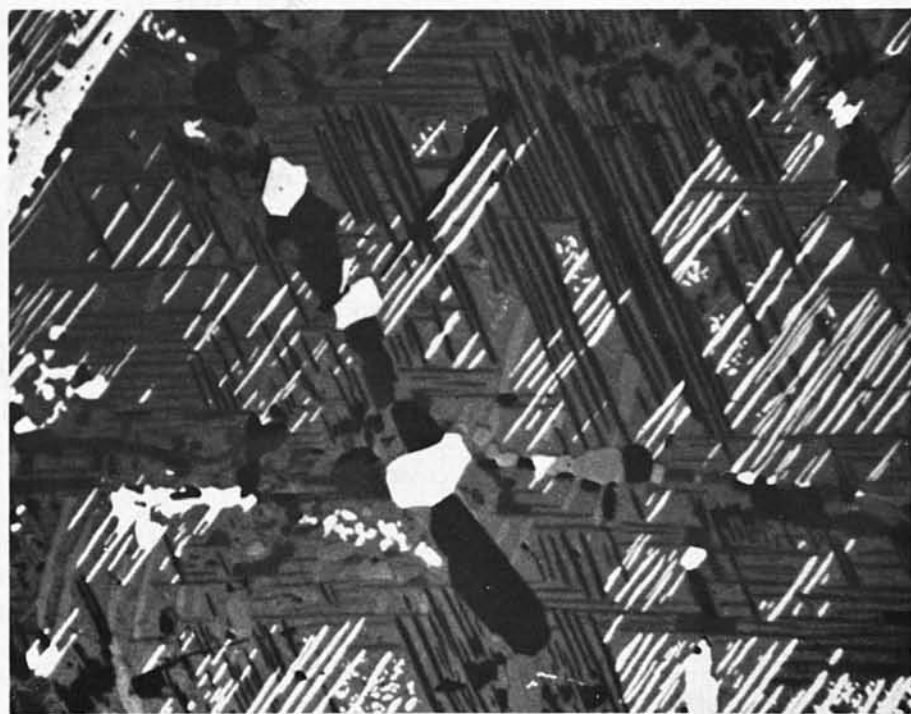

FIGURE 9.9   Exsolution lamellae of ilmenite along (111) planes of host magnetite, Baugstø, Norway (partly crossed polars, width of field = 520 μm).
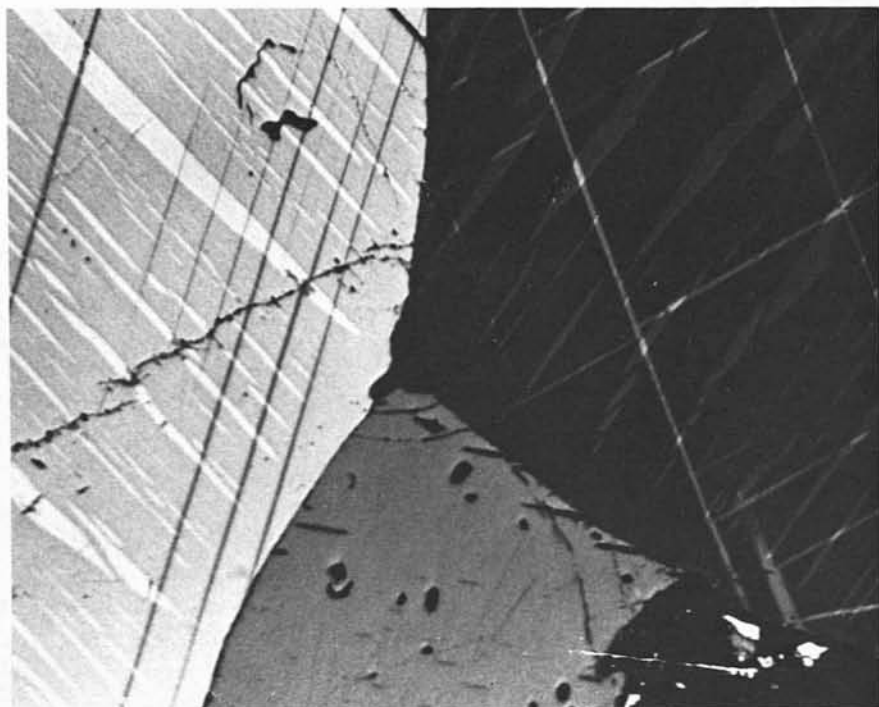
FIGURE 9.10 Lamellar twinning in ilmenite that contains lensoid exsolution bodies of hematite. The twin lamellae extend through both phases, Egersund, Norway (partly crossed polars, width of field = 520 μm).

9.10), a feature that is absent in the associated minerals. Ulvöspinel is slightly darker gray-brown than magnetite and is difficult to distinguish from it unless the two minerals are in contact. Hematite, on the other hand, appears nearly white in comparison with magnetite, ilmenite, or ulvöspinel. It is strongly anisotropic and, if in large enough grains, will display reddish internal reflections. Ilmenite lamellae in magnetite are usually sharp and equal in width throughout their length, but ilmenite lamellae in hematite and hematite lamellae in ilmenite tend to be much more lens-like or pod-like (Figure 9.11). These intergrowths of ilmenite and hematite are extremely striking because of the marked color difference of the phases, and, probably will not be misidentified after they have once been observed.

Phase equilibria among the iron-titanium oxides (Figure 9.12) were determined by Buddington and Lindsley (1964), who found that the solubility of ilmenite in magnetite is much too small, even up to magmatic temperatures, to account for most ilmenite-magnetite intergrowths by simple exsolution. They concluded that subsolidus oxidation of magnetite-ulvöspinel with subsequent formation of the ilmenite-hematite lamellae takes place during cooling of many igneous and metamorphic rocks. They further found that coexisting
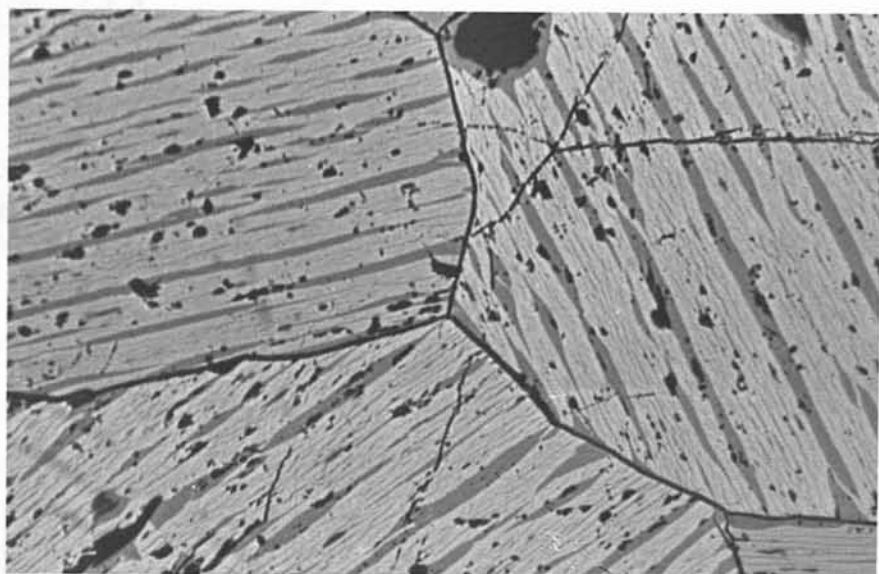
FIGURE 9.11 Lens-like exsolution bodies of ilmenite in hematite at the intersection of three grains, Wilson Lake, Labrador (width of field = 520 μm).
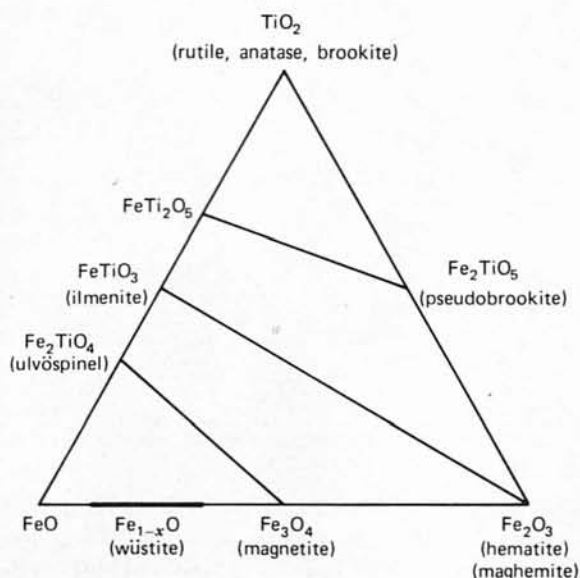

TiO$_2$
(rutile, anatase, brookite)

FeTi$_2$O$_5$

FeTiO$_3$
(ilmenite)

Fe$_2$TiO$_5$
(pseudobrookite)

Fe$_2$TiO$_4$
(ulvöspinel)

FeO

Fe$_{1-x}$O
(wüstite)

Fe$_3$O$_4$
(magnetite)

Fe$_2$O$_3$
(hematite)
(maghemite)

FIGURE 9.12 Phases in the system FeO-Fe$_2$O-TiO$_2$ showing the major solid solution series magnetite-ulvöspinel, hematite-ilmenite, and pseudobrookite-FeTi$_2$O$_5$. Compositions are in mole percent. (From A. F. Buddington and D. Lindsley, *J. Petrol.* **5**, 311, 1964; used with permission.)

223

equilibrated pairs of titaniferous magnetite and ilmenite may permit simultaneous determination of the temperature and oxygen fugacity at the time of formation. The compositions of coexisting magnetite-ulvöspinel (solid lines) and ilmenite-hematite (dashed lines) as functions of temperature and oxygen fugacity are shown in Figure 9.13.

Titaniferous magnetites occur in a wide variety of rocks (Figure 9.14) and should always be carefully examined for the presence of exsolution lamellae. Application of the relationships illustrated in Figure 9.13 to determine temperature requires that the grains be of primary origin and that their compositions not be altered by secondary exsolution. Occasionally, small amounts of magnetite occur as exsolution-like lamellae within ilmenite-hematite; this apparently results from late-stage small-scale reduction.
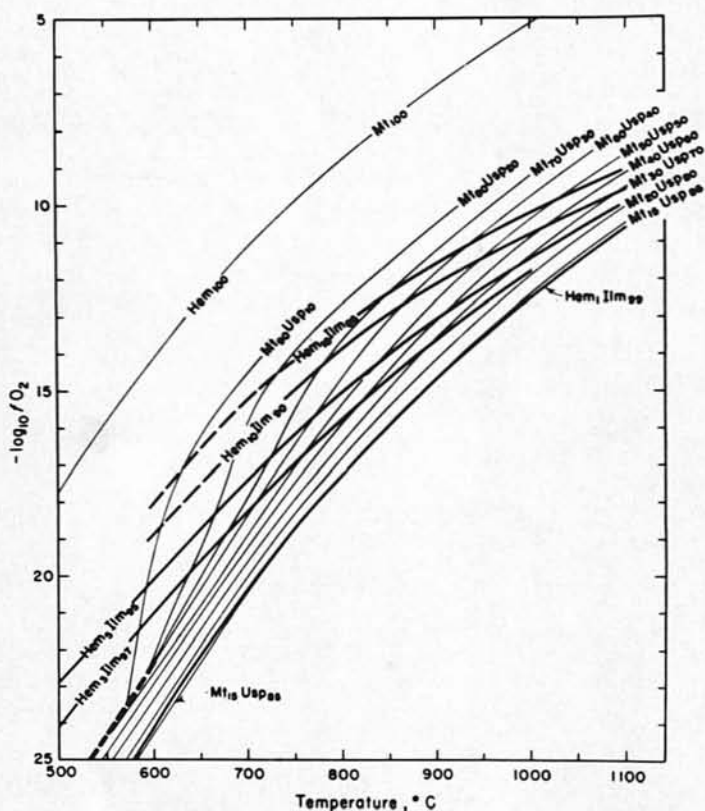

FIGURE 9.13 Projection onto the fO_2-T plane of conjugate surfaces in fO_2-T-X space. The projection is parallel to two composition axes, magnetite-ulvöspinel$_{ss}$, and the coexisting hematite-ilmenite$_{ss}$, so that intersecting contours are the projection of tie lines connecting conjugate pairs. The temperature-composition relations of the magnetite-ulvöspinel solvus are shown in the heavy dashed line. The hematite-ilmenite solvus (not shown) lies between the curves Hem$_{100}$ and Hem$_{15}$Ilm$_{85}$. Compositions are in mole percent. (From A. F. Buddington and D. Lindsley, *J. Petrol.* **5**, 316, 1964; used with permission.)
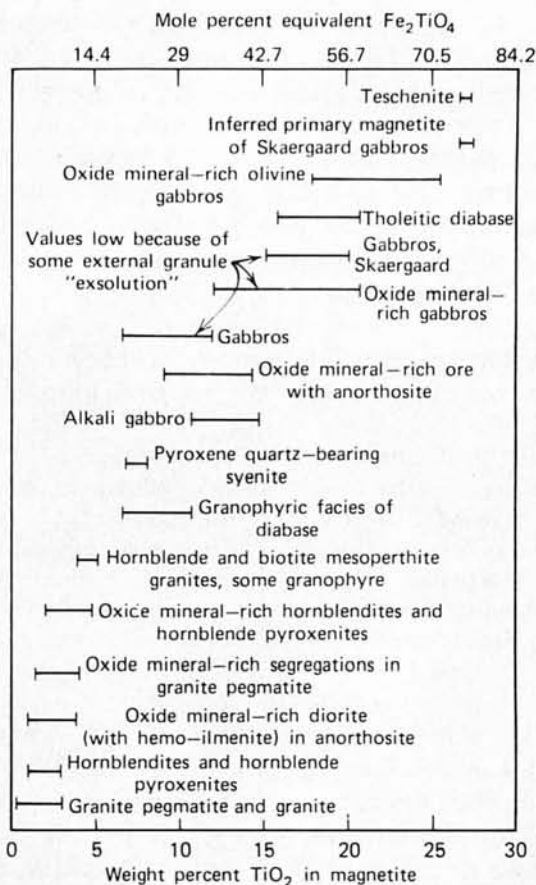
FIGURE 9.14 Range of TiO_2 and equivalent Fe_2TiO_4 contents in magnetites of some plutonic and hypabyssal rocks. (From A. F. Buddington and D. Lindsley, *J. Petrol.* **5**, 342, 1964; used with permission.)

Titaniferous magnetites commonly contain up to several percent vanadium, chromium, and aluminum substituting for Fe^{3+}, and manganese and magnesium substituting for Fe^{2+}. Where magnetite and ilmenite have developed as a coexisting pair, the magnetite contains more V, Cr, and Al but less Mn and Mg than the ilmenite.

The oxidation of ilmenite and titaniferous magnetite leads to the development of rims and a complex variety of lamellar intergrowths of these phases with rutile, pseudobrookite, and titanohematite. The stages of development have been exhaustively described and illustrated by Haggerty [in Rumble (1976) and Lindsley (1991)].

9.4.2 Origin of the Ores

The dispersed grains of titaniferous magnetite and ilmenite in igneous rocks appear to be normal accessories that have crystallized along with the host

silicates. However, the origin of the massive magnetite-ilmenite ores is not well understood but appears to be the result of fractionation from mafic complexes. The suggested modes of origin include the following.

Fractional Crystallization and Gravitative Differentiation This mechanism, which accounts for the formation of many early formed silicates in differentiating intrusions and for many chromite ores (see Section 9.2), appears to explain satisfactorily many aspects of the iron-titanium oxide layers in such complexes as the Duluth gabbro.

Residual Liquid Segregation The process of residual liquid segregation has been summarized by Bateman (1951, p. 406) as follows:

> With progressive crystallization and enrichment of the residual liquid, its density would come to exceed that of the silicate crystals and its composition might reach the point of being chiefly oxides of iron and titanium. . . . At this stage three possibilities may occur: final freezing may occur to yield a basic igneous rock with interstitial oxides . . . [and] the residual liquid may he filter pressed out of the crystal mush and be injected elsewhere; or the enriched residual liquid may drain downward through the crystal interstices and collect below to form a gravitate liquid accumulation.

The relationships of many large accumulations of Fe-Ti oxide layers, as in the Bushveld Complex, and of discordant bodies, as in the Adirondacks, are consistent with this mechanism. Limited experimental investigations in the system magnetite-apatite-diorite (Philpotts, 1967) suggest that there is an eutectic at two-thirds oxide to one-third fluorapatite—a composition that is very similar to that found in some anorthositic oxide concentrations. These findings lend some support to a possible residual liquid segregation mechanism for the formation of iron-titanium oxide ores. A third mechanism that has been suggested is that of *metamorphic migration.* Liberation of iron and titanium from sphene, biotite, hornblende, and titanaugite, and subsequent migration and concentration during granulite facies metamorphism have also been suggested as a possible mechanism to form iron-titanium oxide masses. Considerable granulation of iron-titanium oxide grains is common, but there is little evidence of massive replacement.

9.5 COPPER/MOLYBDENUM SULFIDES ASSOCIATED WITH PORPHYRITIC INTRUSIVE IGNEOUS ROCKS ("PORPHYRY COPPER/ MOLYBDENUM" DEPOSITS)

Mineralogy

Major	Pyrite, chalcopyrite, molybdenite, bornite
Minor	Magnetite, hematite, ilmenite, rutile, enargite, cubanite, cassiterite, huebnerite, gold
Secondary	Hematite, covellite, chalcocite, digenite, native copper

Mode of Occurrence   Sulfides are present in veinlets and as disseminated grains in, or adjacent to, porphyritic intrusions ranging in composition from quartz diorite to quartz monzonite. The host porphyry and adjacent rocks are commonly altered in concentric siliceous, potassic, phyllic, argillic, and propylitic zones.

Examples

Copper	Bisbee, Ray, Ajo, Arizona; Butte, Montana; Bingham Canyon, Utah; El Salvador, El Teniente, Chuquicamata, Braden, Chile; Bethlehem, Endako, British Columbia; Ok Tedi, Papua-New Guinea; Cananea, Mexico
Molybdenum	Climax, Urad, Henderson, Colorado; Questa, New Mexico; Quartz Hill, Alaska

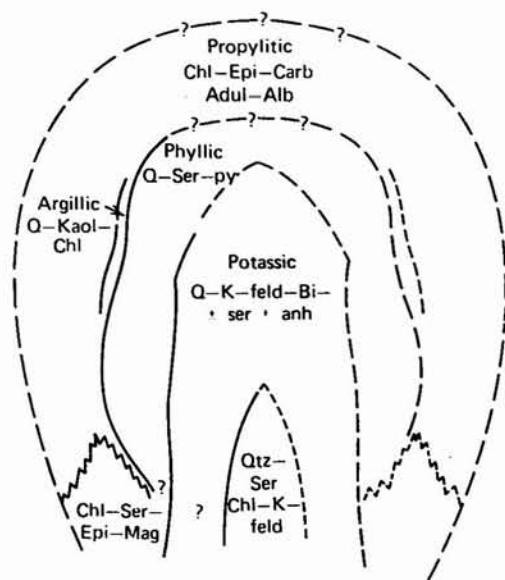### 9.5.1 Mineral Zoning in Porphyry Copper Deposits

Porphyry deposits of this type now constitute the world's primary sources of copper and molybdenum and also serve as significant producers of several other base metals, gold, and silver. These deposits are concisely summarized in the definition given by Lowell and Guilbert (1970, p. 374) as follows:

> A copper and/or molybdenum sulfide deposit consisting of disseminated and stockwork veinlet sulfide mineralization emplaced in various host rocks that have been altered by hydrothermal solutions into roughly concentric zonal patterns [Figure 9.15a]. The deposit is generally large, on the scale of thousands of feet . . . and . . . is associated with a complex, passively emplaced, stock of intermediate composition including porphyry units.

The low grades of these deposits—0.5–0.8% Cu and 0.02% Mo for a typical porphyry copper, and 0.3% Mo and 0.05% Cu for a typical porphyry molybdenum—evidence the dispersed nature of the sulfides. Pyrite is generally the most abundant sulfide and may occur in association with the other sulfides or alone in barren quartz veinlets. In copper-dominant porphyry deposits, the total sulfide distribution and relative amounts of the economic minerals follow a concentric pattern coaxial with the alteration zones, as shown in Figure 9.15b and discussed below.

Potassic Zone   The inner zone of potassic alteration commonly coincides with two zones of mineralization:

1. An inner low-grade (<0.3% Cu) core characterized by pyrite and chalcopyrite in a ratio of roughly 1:2, minor magnetite and minor molybdenite.
2. An ore shell (>0.5% Cu), in which the pyrite to chalcopyrite ratio is
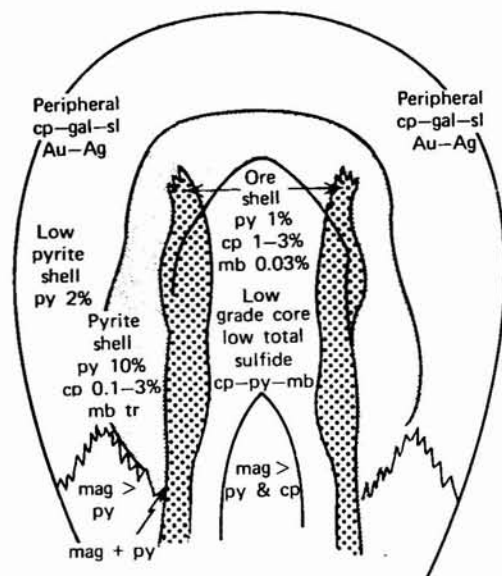
FIGURE 9.15 Idealized diagram showing concentric alteration-mineralization zones occurring in porphyry copper deposits: (a) alteration zones; (b) mineralization zones. (After J. D. Lowell and J. M. Guilbert, *Econ. Geol.* **65**, 379, 1970; with permission of the publisher.)

roughly 1:1 and each mineral constitutes about 1% of the rock. Small amounts of molybdenite are present in veinlets and as dispersed grains. Bornite, as discrete grains and intimately intergrown with the chalcopyrite, is common in small amounts.

Phyllic and Argillic Zones   The phyllic zone coincides with the outer portion of the "ore shell" and the surrounding low-grade portion of the "pyrite shell" in which copper grade decreases to 0.1–0.5%. The pyrite-to-chalcopyrite ratio is roughly 10:1, and pyrite may constitute as much as 10% of the rock volume as coarse (0.5 mm) subhedral vein fillings and disseminated grains. The outer part of the "pyrite shell" contains up to 25% pyrite in the form of coarse anhedral pyritic-quartz veins up to 2 cm thick.

Propylitic Zone   In the propylitic zone, the outer zone of the ore body, mineralization consists of pervasive pyrite in veinlets (2–6% of the rock) and local small veins containing typical hydrothermal base-metal assemblages, such as the pyrite-chalcopyrite-galena-sphalerite-tetrahedrite associations discussed in Section 9.6. The zonal structure of these deposits means that the level of erosion can have an important influence on the geology and mineralogy of the exposed portion of deposits, as noted by Sillitoe (1973).

Molybdenum-rich deposits such as Climax and Henderson, Colorado, exhibit an umbrella-like shape emplaced in or about the intrusion core (Figure 9.16). In the Climax deposit, the mineralization occurs in two crudely
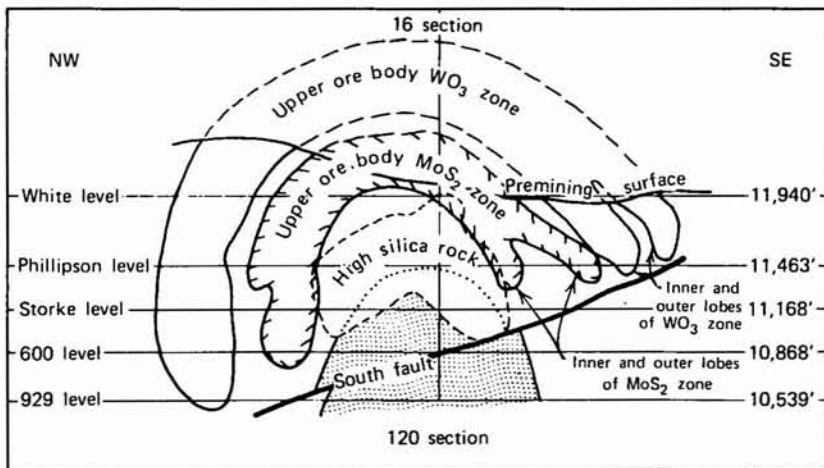

FIGURE 9.16   Generalized cross section of the Upper Ore Body at Climax, Colorado. This illustrates the concentric nature of the mineralized zones about the intrusion. (Reproduced with permission from *Ore Deposits of the United States 1933/1967*, Am. Inst. Min. Metall. Petrol. Eng., p. 628.)

concentric zones—an outer tungsten zone and an inner molybdenum zone. The hydrothermal alteration in and near the ore bodies consists of potassium feldspar, sericite, fluorite, and topaz, with minor amounts of biotite, chlorite, and epidote.

9.5.2 Ore Mineral Textures

The ore minerals of the porphyry copper deposits occur in veinlets or as disseminated grains, as shown in Figures 9.17 and 9.18. Pyrite is the dominant sulfide and is present as anhedral to euhedral grains in both types of occurrences. Chalcopyrite is the dominant copper mineral, occurring as anhedral interstitial grains and as fracture fillings in pyrite. Bornite is present as discrete anhedral grains with the pyrite and chalcopyrite and as both exsolution and oxidation lamellae within chalcopyrite. In near-surface ores, covellite, chalcocite, and digenite are commonly observed forming secondary alteration rims on chalcopyrite and bornite; native copper is sometimes present. Molybdenite is present in significant amounts in the molybdenum-rich porphyry deposits but is minor in many copper-rich examples. The molybdenite is generally observed as subparallel to crumpled blades disseminated in veinlets.

In molybdenum-rich ores such as those at Climax, Colorado, the molybdenite is present as random to subparallel tiny (<0.1 mm) hexagonal plates embedded in the vein-filling quartz. Tungsten in these ores is present as small
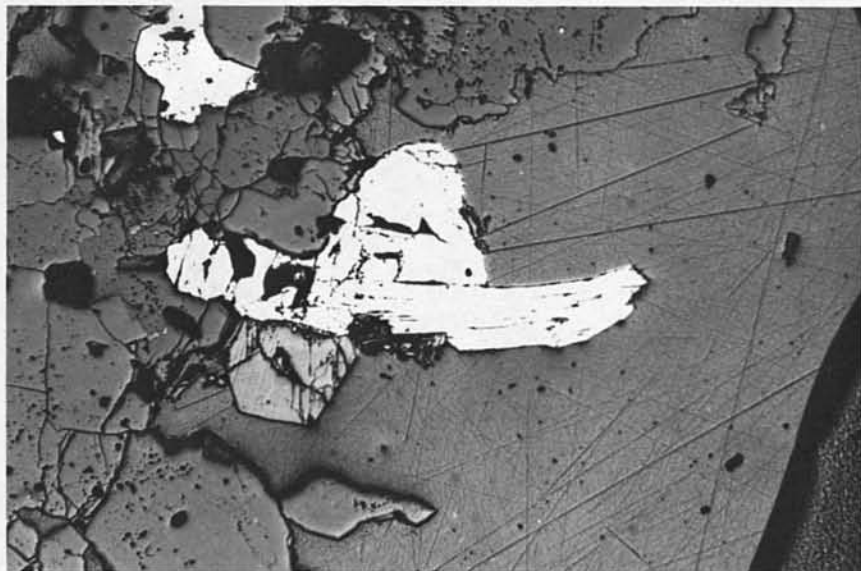

FIGURE 9.17 Molybdenite lath with associated anhedral grain of chalcopyrite, Bingham Canyon, Utah (width of field = 520 μm).
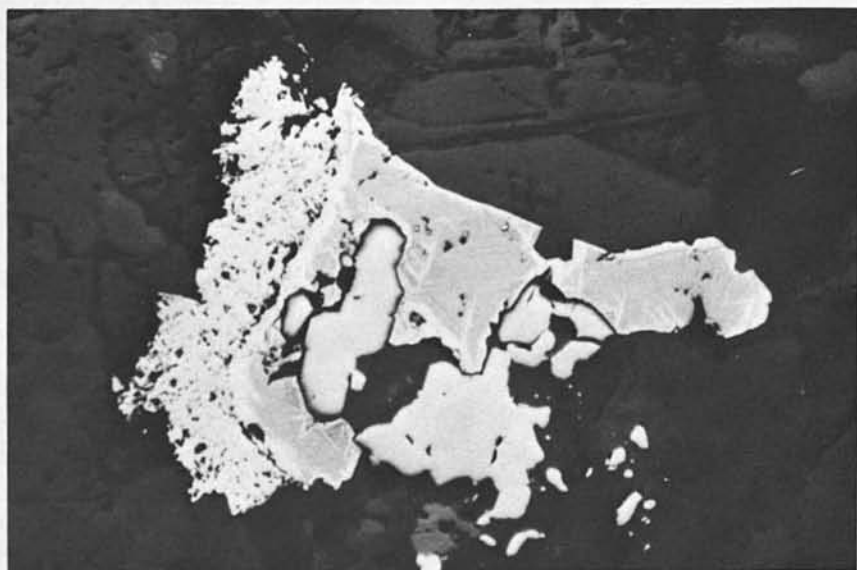
FIGURE 9.18   Central grain of rutile surrounded by bornite that shows marginal laths and rim of chalcopyrite. A polycrystalline mass of enargite is seen to the left of the field of view, Bingham Canyon, Utah (width of field = 520 μm).

irregularly distributed euhedral huebnerite grains in pyrite-quartz-sericite veinlets.

Enargite is occasionally present in porphyry ores as anhedral grains (Figure 9.18) or as rims on the copper-iron sulfides. Cubanite is rare but has been observed as exsolution lamellae within chalcopyrite.

9.5.3 Origin of the Ores

The genesis of porphyry-type deposits has been the subject of considerable study and remains, in part, conjectural. All of these deposits occur within, or very close to, orogenic zones; however, it appears that there is a distinction between the two major types, with Cu-bearing porphyries lying along consuming plate margins and Mo-bearing porphyries being typical of tensional (rifting) environments. Sillitoe (1972) has suggested that the porphyry bodies represent partially melted oceanic rocks that have transported metals originally emplaced at midoceanic ridges, subducted, and then emplaced along continental margins. Mitchell and Garson (1972) have described the mechanism:

Porphyry copper deposits are emplaced in igneous belts located either on continental margins or in island arcs. These belts are related to partial melting of wet oceanic crust descending along Benioff zones at depths of 150–250 km. Deposition of the copper occurs where metal-carrying solutions rising from the descending crust meet meteoric brines.

Although this general model fits the South American and the Pacific Island arc deposits, it is difficult to reconcile with settings of many southwestern United States and Rocky Mountain occurrences (Lowell, 1974). Nevertheless, there is general agreement on the mode of emplacement once a magma has been generated. The emplacement of a porphyritic magma to within 0.5–2 km of surface establishes convective motions in the adjacent ground water system if the surrounding rocks have reasonable permeability. Hot, chemically potent solutions rise above the stock as new, initially cool, solutions circulate in toward the stock. As a result of the cooling, the outer shell crystallizes; the shell is subsequently highly fractured by pressure building up from H_2O released from the crystallizing magma. The central core is quenched to a porphyry, cut by a stockwork of quartz and quartz-feldspar veinlets as heat is rapidly lost to the ground water system. Precipitation of the sulfides and quartz in these veins occurs at temperatures as high as 725°C in the potassic zone and around 300–390°C in the argillized zone.

Fluid inclusion studies by several workers (e. g., Roedder, 1971; Moore and Nash, 1974; Hall, Friedman, and Nash, 1979) have shown that the fluids that deposited ores in the cores of copper-molybdenum deposits were highly saline (often containing more than 60% salts), underwent extensive boiling, and were trapped at temperatures up to 725°C. In some deposits, distinct zones of the hypersaline inclusions correlate not only with the ore zones but also specifically with the fracture systems believed responsible for the introduction of the metals.

9.6 COPPER-LEAD-ZINC-SILVER ASSEMBLAGES IN VEIN DEPOSITS

Mineralogy

|	
Major	Pyrite, sphalerite, galena, chalcopyrite, tetrahedrite
Minor	Bornite, chalcocite, enargite, argentite, gold, hematite, pyrrhotite, proustite-pyrargyrite, Pb-Bi-Sb-sulfosalts
Secondary	Cerussite, anglesite, goethite, smithsonite, azurite $[Cu_3(CO_3)_2(OH)_2]$, malachite $[Cu_2(CO_3)(OH)_2]$, argentite, covellite, chalcocite, silver, and many other phases
Associated Gangue Minerals	Quartz, calcite, dolomite, barite, fluorite, rhodochrosite, siderite, chlorite, sericite

Mode of Occurrence   Copper-lead-zinc-silver sulfide ores occur as hydrothermal vein fillings and replacement (usually of limestone) bodies often associated with intermediate to acid intrusions.

Examples   Especially prominent in the North American Cordillera—Creede, Gilman, Leadville, Colorado; Tintic, Park City, Utah; Eureka, Nevada; Bluebell, British Columbia; Zacatecas, Mexico; Eastern Transbaikalia, Russia; Casapalca, Peru.

9.6.1 Mineral Associations and Textures

Copper-lead-zinc-silver vein deposits are characterized by coarse-grained (1 mm–2 cm), banded to massive aggregates of pyrite, galena, sphalerite, and chalcopyrite (Figure 9.19). The bulk mineralogy is thus similar to that of massive stratabound sulfide deposits except that galena tends to be much more abundant in the vein deposits. Pyrite, sphalerite, and gangue minerals such as quartz, calcite, and fluorite often tend to be euhedral with the development of well-formed faces. Galena is coarse-grained and may be present as anhedral polycrystalline aggregates interstitial to pyrite and sphalerite or as well-formed crystals. Tetrahedrite is common in small amounts and is very important as a major carrier of silver, the content of which varies directly with the Sb/As ratio. The tetrahedrite is usually present as small rounded blebs within or along the margins of galena grains (Figure 9.19b). Many ores of this type exhibit complex paragenesis in which multiple episodes of deposition, deformation, leaching, and replacement are evident. Incipient oxidation is evidenced by the formation of covellite or chalcocite along fractures in chalcopyrite.

The deposition of these ores in open fractures has often led to the formation of distinct bands, commonly monomineralic, parallel to walls of the fracture. Mineral growth in these bands can be seen either as colloform ribbons or as well-faceted subhedral crystals. Changes in the nature of the ore fluid during deposition are reflected not only in the changing mineralogy of subsequent bands and in mineralogic variations along a vein system but also in the presence of growth zoning in individual crystals. This zoning is evident in many sulfides as rows of small inclusions or differences in polishing hardness and color, but is especially evident in coarse-grained sphalerites as distinct color bands (see Figure 7.4), which are visible if doubly polished thin sections are examined. In general, though not in every case, darker sphalerite bands are richer in iron than are lighter bands; the FeS content varies widely (0.5–20 mol %) even in individual crystals. Sphalerites in these deposits frequently contain crystallographically oriented rows of chalcopyrite blebs ($\sim$20–100 µm), which have been appropriately referred to as "chalcopyrite disease" (see Section 7.5). Some of these small blebs (as they appear in polished surfaces) are actually worm-like rods that may extend for several millimeters within a crys-
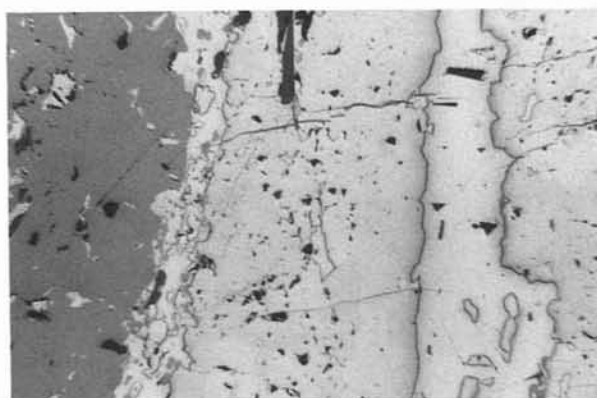
(a)
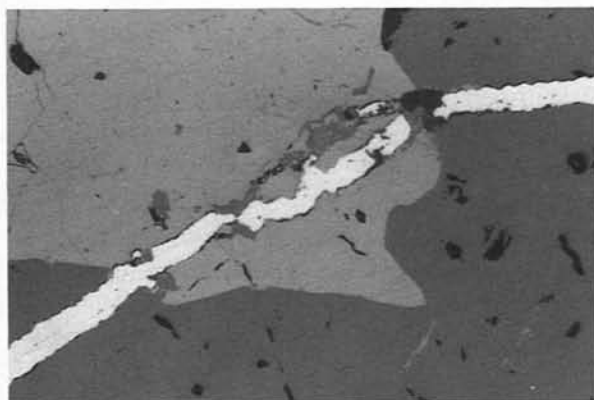
(b)

FIGURE 9.19 (a) Typical base-metal vein ore with sequential zones (from left to right) of sphalerite, galena, pyrrhotite, galena, and pyrrhotite, Naica Mine, Mexico (width of field = 1,200 μm). (b) Veinlet of native silver (white), which cuts across, and thus postdates, chalcopyrite (light gray) and bornite (dark gray), San Martin Mine, Mexico (width of field = 1,200 μm).

tal. The chalcopyrite apparently forms by epitaxial growth, replacement, or by reaction of copper-bearing fluids with iron-bearing sphalerite.

Fluid inclusion studies of hydrothermal vein deposits (Roedder, 1979) have revealed homogenization temperatures from 100–500°C and salinities that are generally less than 10 wt % NaCl equivalent. Detailed work on the Creede, Colorado, ores (Roedder 1977) yields homogenization temperatures of 200–270°C in 20 recognizable stratigraphic growth zones of sphalerite. The color zonation in these sphalerites (Figure 7.4) apparently corresponds to abrupt changes in the nature of the ore fluids as indicated by the fluid inclusions.

9.6.2 Supergene Alteration

Near-surface portions of these ores often reveal moderate to extensive altera-
tion by meteoric waters. The oxidation of pyrite causes the formation of sul-
furic acid and ferrous sulfate, which results in the breakdown of other sulfides.
The end result is that the uppermost parts of the veins consist of a boxwork
gossan of iron oxides and hydroxides. At lower levels, secondary covellite,
chalcocite, galena, and sometimes silver have been reprecipitated. Also much
in evidence are secondary carbonates, sulfates, and silicates of copper, lead,
and zinc.

9.6.3 Origin of the Ores

Copper-lead-zinc-silver vein deposits apparently form as a result of circulat-
ing hydrothermal fluids that extract, transport, and then precipitate sulfide
minerals as open-space fillings and replacements. Studies of fluid inclusions,
wall-rock alteration, and the sulfide ore minerals indicate that the ore-forming
fluids were chloride-rich brines (see Chapter 8), often containing a large and
sometimes episodically introduced component of recirculated meteoric
water, which precipitated the sulfides in response to a decrease in temperature,
a decrease in pressure (which may sometimes allow boiling), reaction with
wall rocks, or mixing with other fluids. Metals originally derived from mag-
matic sources or from country rocks were probably transported as chloride or
possibly sulfide complexes. The manner in which the sulfur of the ore min-
erals was transported is not known with certainty, but most workers believe
that sulfate was the dominant form. Barnes (1979), however, has made out a
strong case for transport of considerable metal as sulfide complexes. The flow
of hot (150–300°C) reactive fluids commonly results in alteration haloes rich
in quartz, feldspar, and sericite, as described by Meyer and Hemley (1967) and
Rose and Burt (1979).

9.7 THE SILVER-BISMUTH-COBALT-NICKEL-ARSENIC (-URANIUM) VEIN ORES

Mineralogy   Very complex mineral assemblages, often with 30 or 40 different
opaque minerals reported from a single deposit.

Major Phases   May include native silver, native bismuth, niccolite,
                     skutterudite, rammelsbergite, safflorite, löllingite,
                     cobaltite, gersdorffite, and arsenopyrite, along with
                     such common sulfides as pyrite, marcasite,
                     chalcopyrite, and galena. Certain deposits contain
                     substantial uranium as uraninite often associated
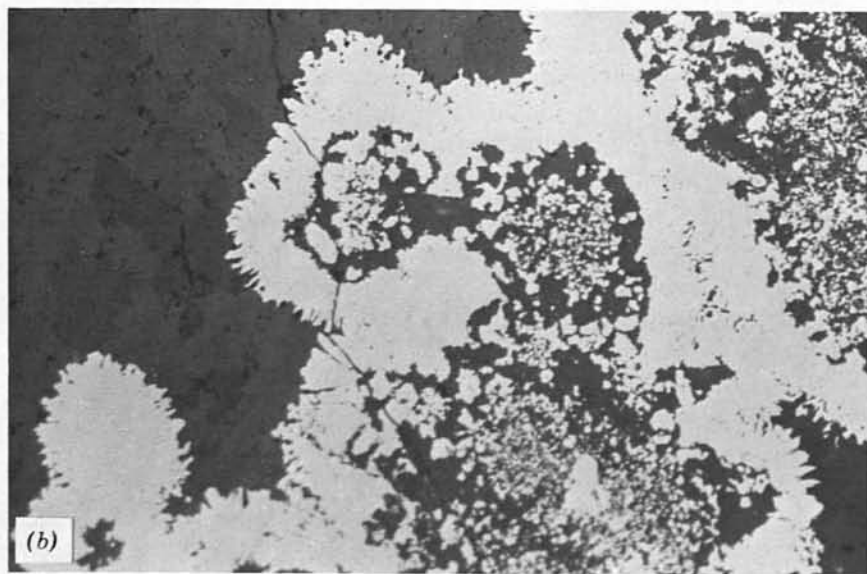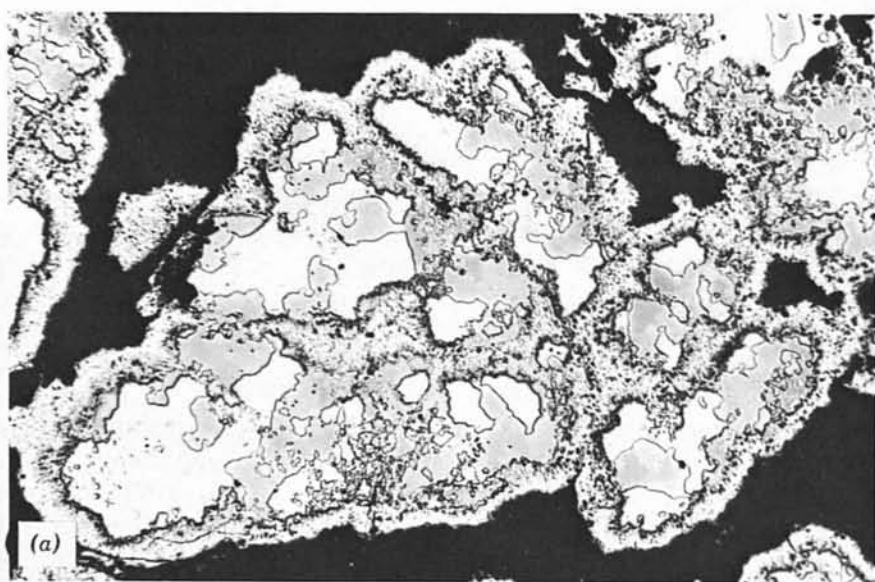   with hematite

FIGURE 9.20 Vein ores from Cobalt, Ontario, Canada. (*a*) Dendritic silver surroun-
ded by breithauptite (medium gray) and cobaltite (width of field = 2,000 μm). (*b*)
Cobaltite showing colloform textures (width of field = 2,000 μm).

Other Phases   (Which may locally achieve economic importance)
                        include a large number of other Fe, Co, Ni in
                        combination with S, As, Sb minerals, sulfides, and
                        sulfosalts, particularly of silver (some of which are
                        listed in Figures 9.21 and 9.22)
Gangue Phases   Carbonates and quartz

Mode of Occurrence   The ores occur in veins that are mostly fissure fillings
of fault and joint planes. Commonly, the veins range from a few centimeters to
several meters in thickness and occur in a considerable variety of host rocks
(quartzites, greywackes, conglomerates, slates, schists, diabases, and granites,
for example) ranging in age through most of the geological time scale.

Examples   The most famous examples occur in the Cobalt-Gowganda area,
Ontario, Canada. Others include Great Bear Lake, N.W.T., Canada; the
Erzgebirge, Germany; Kongsberg, Norway; Jachymov, Czechoslovakia.

9.7.1   Mineral Assemblages, Textures, and Paragenesis

The ores of this type are characterized by both very complex mineral assem-
blages and the presence of delicate zonal and dendritic textures. For example,
native silver commonly occurs in dendritic patterns that are surrounded by
arsenides (Figure 9.20a) in rounded patterns termed "rosettes." Colloform tex-
tures are also commonly developed (Figure 9.20b) involving the native metals
and arsenides. Frequently, these accretionary structures are slightly disrupted
with introduction of later veining materials, and periods of direct deposition
are interspersed with phases of replacement. The combination of these proc-
esses with the complex assemblages has enabled ore microscopists to unravel
long, complex paragenetic sequences for these ores. The study of the Cobalt,
Ontario, ores (Figure 9.21) by Petruk (1971a) and of the Great Bear Lake
deposits (Figure 9.22) by Badham, Robinson, and Morton (1972) are good
examples.
    At Cobalt, Petruk (1971a) has subdivided the arsenide assemblages into Ni-
As, Ni-Co-As, Co-As, Co-Fe-As, and Fe-As types, with Co-As being most
abundant. Native silver is the main native metal and occurs as cores to
arsenide rosettes, as veinlets in arsenides and carbonates, and in association
with sulfides. Silver at the cores of rosettes has been interpreted by Petruk
(1971a) as being the earliest mineral in the ore, with the arsenides being
deposited around it later. In contrast, Scott (1972) interprets much of the silver
in the cores of the rosettes as being a later replacement of the arsenides. The
veinlet silver in arsenides and carbonates is interpreted as being a late variety
and that associated with sulfides, as being even later. The high-grade silver ore
is associated with parts of the veins containing Ni-Co-As and Co-As assem-
blages. The sulfides occur as disseminated grains, veinlets, and colloform
masses in the veins and the wall rocks. On the basis of their textural rela-
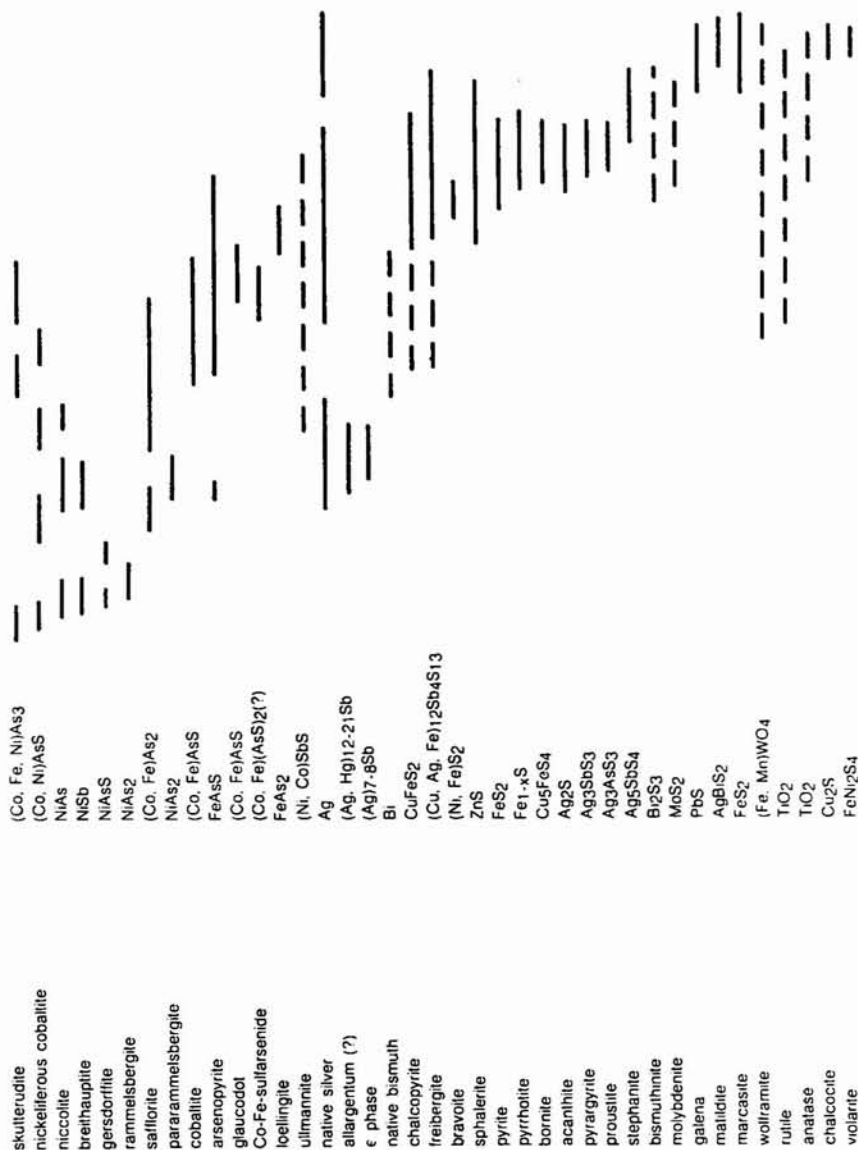
skutterudite — (Co, Fe, Ni)As3
nickelliferous cobaltite — (Co, Ni)AsS
niccolite — NiAs
breithauptite — NiSb
gersdorffite — NiAsS
rammelsbergite — NiAs2
safflorite — (Co, Fe)As2
pararammelsbergite — NiAs2
cobaltite — (Co, Fe)AsS
arsenopyrite — FeAsS
glaucodot — (Co, Fe)AsS
Co-Fe-sulfarsenide — (Co, Fe)(AsS)2(?)
loellingite — FeAs2
ullmannite — (Ni, Co)SbS
native silver — Ag
allargentum (?) — (Ag, Hg)12-21Sb
ε phase — (Ag)7-8Sb
native bismuth — Bi
chalcopyrite — CuFeS2
freibergite — (Cu, Ag, Fe)12Sb4S13
bravoite — (Ni, Fe)S2
sphalerite — ZnS
pyrite — FeS2
pyrrhotite — Fe1-xS
bornite — Cu5FeS4
acanthite — Ag2S
pyrargyrite — Ag3SbS3
proustite — Ag3AsS3
stephanite — Ag5SbS4
bismuthinite — Bi2S3
molybdenite — MoS2
galena — PbS
matildite — AgBiS2
marcasite — FeS2
wolframite — (Fe, Mn)WO4
rutile — TiO2
anatase — TiO2
chalcocite — Cu2S
violarite — FeNi2S4

FIGURE 9.21 Mineral assemblage and approximate paragenetic sequence in the Silver-fields Deposit, Cobalt, Ontario. (After Petruk, 1968.)
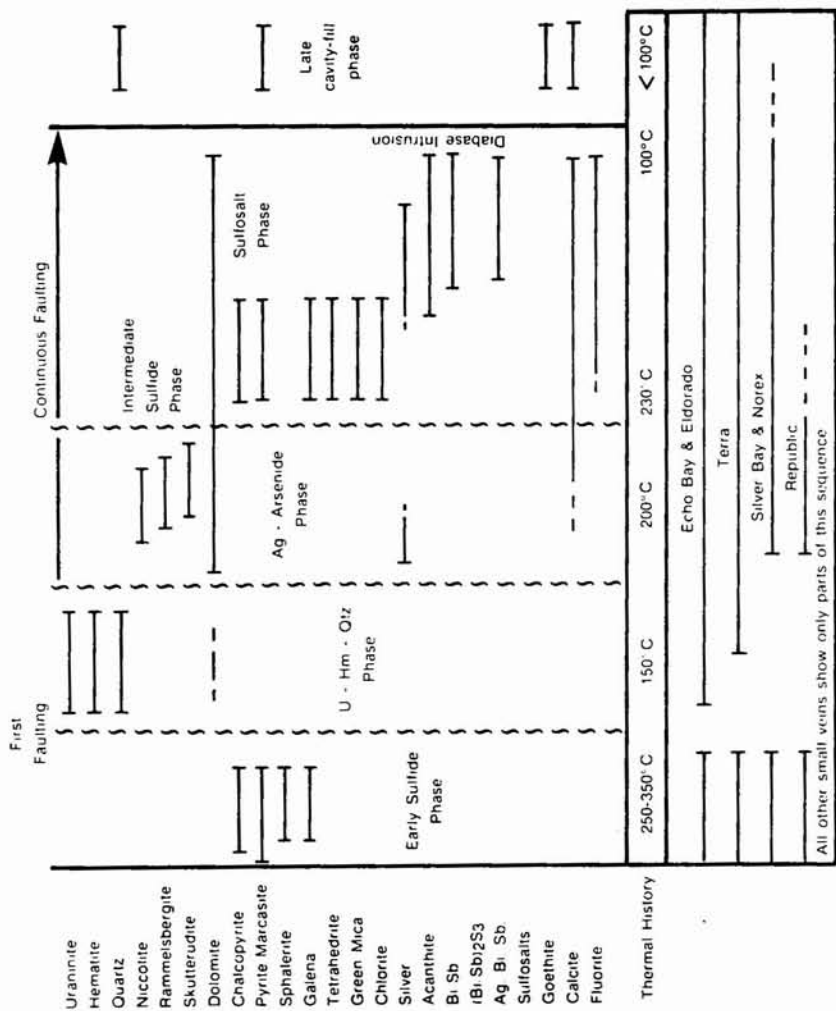
FIGURE 9.22 The paragenetic sequence, phases, and estimated temperatures of mineralization at Great Bear Lake, Northwest Territories. Also shown are the stages of mineralization occurring in particular mines and veins. (After Badham et al., 1972.)

239

tionships, it is suggested that most of the sulfides were in the rocks prior to ore deposition and were remobilized and redeposited in and around the veins during mineralization. Some sulfides may also represent a late stage of the main mineralization process. The paragenetic sequence determined by Petruk (1968) for ore formation at the Silverfields Mine, Cobalt, is illustrated in Figure 9.21.

The mineral assemblages at Great Bear Lake differ from those at Cobalt by the presence of significant uranium mineralization in the form of uraninite. Again, a complex assemblage and sequence of deposition and replacement episodes have been elucidated by ore microscopy. A general paragenetic sequence (after Badham, Robinson, and Morton, 1972) is shown in Figure 9.22. This illustrates that an early phase of sulfide mineralization was followed by uraninite-hematite-quartz mineralization, by nickel and cobalt arsenides, then by silver, by sulfides associated with dolomite, by Ag, Sb, Bi sulfosalts, and by carbonates, quartz, and fluorite. Particular mines may show only a part of this complete mineralization sequence, as indicated in Figure 9.22. Studies of fluid inclusions and sulfur isotopes have made it possible to estimate temperatures of deposition, as noted in that figure.

9.7.2 Mineral Formation

All of the geological, mineralogical, and textural evidence suggests that these ores have been deposited from complex hydrothermal solutions. The sites of deposition were commonly controlled by pre-existing faults and fissures. For the ores of the Cobalt area, Petruk (1971b) has suggested a sequence of depositional temperatures, with early quartz and chlorite deposited at ~200-360°C, arsenide deposition at temperatures around 500-590°C (above the temperature of the rammelsbergite-pararammelsbergite inversion), sulfides deposited at 400-200°C, and later gangue phases and sulfides below 200°C. Scott and O'Connor (1971) have examined two populations of fluid inclusions in ore vein quartz in the Cobalt Camp and have determined depositional temperatures of 195-260°C and 285-360°C. Scott (1972) has calculated the temperature gradients adjacent to the diabase sheet at Cobalt and has concluded that the maximum temperature of ore deposition would have been 535°C. The depositional temperatures for the Great Bear Lake deposits have already been indicated in Figure 9.22. For the Echo Bay Mines, the main mineralization temperatures range between 230°C and 100°C (Badham, Robinson, and Morton, 1972). Information on the chemical nature of the ore fluids has also been obtained from fluid inclusion and stable isotope studies.

The origin of the solutions producing deposits of this type is still very much a matter of debate. Origin of the Cobalt area ores is commonly linked with a diabase intrusion (Jambor, 1971), although, for ores of this general type, four possible sources have been invoked (Halls and Stumpfl, 1972).

1. Direct hydrothermal evolution from granitic intrusions
2. Direct hydrothermal evolution from basic intrusions

3. Hydrothermal processes causing selective concentration from associated black shales or pre-existing sulfide deposits
4. Ore solutions from a deep source near the crust-mantle boundary

9.8 TIN-TUNGSTEN-BISMUTH ASSEMBLAGES IN VEIN DEPOSITS

Mineralogy

Major	Cassiterite, arsenopyrite, wolframite, bismuthinite, pyrite, marcasite, pyrrhotite
Minor	Stannite, chalcopyrite, sphalerite, tetrahedrite, pyrargyrite, bismuth, galena, rutile, gold, franckeite, molybdenite
Gangue	Quartz, tourmaline, apatite, fluorite.

Mode of Occurrence Tin-tungsten-bismuth ores occur as open-space hydrothermal vein fillings that show several stages of vein growth. The hydrothermal veins are usually associated with granitic stocks or batholiths.

Examples Panasqueira, Portugal; Llallagua, Tasna, Colcha, Huanuni, Sayaquira, Oruro, and Potosi Districts, Bolivia; Cornwall tin district, S.W. England.

9.8.1 Mineral Associations and Textures

Tin-tungsten-bismuth ores occur as open-space hydrothermal vein fillings, commonly formed from several stages of mineralization. The earliest stage is dominated by quartz and cassiterite but may also contain considerable tourmaline, bismuthinite, arsenopyrite, apatite, and wolframite. The following stage typically contains pyrrhotite, sphalerite, chalcopyrite, and stannite, and may also contain franckeite, cassiterite, arsenopyrite, and silver-bearing minerals such as tetrahedrite, matildite, and proustite-pyrargyrite. Later stages of vein development involve the alteration of pyrrhotite to pyrite, marcasite, and siderite, minor deposition of sphalerite, and the formation of hydrous phosphates.

Early vein minerals such as quartz, cassiterite, and bismuthinite typically occur as prismatic crystals and blades that may line the vein walls or may occur as radiating bundles (see Figure 8.11a). Quartz usually forms a course band on the vein walls, with cassiterite and bismuthinite making up the central portion of the veins. Wolframite may be present as euhedral to subhedral granular masses that overgrow quartz and cassiterite. Native bismuth may occur as alteration blebs in bismuthinite and as small patches with arsenopyrite, which occurs as veinlets and scattered euhedra (Figure 9.23a).

Pyrrhotite and sphalerite may infill space between quartz and cassiterite crystals (see Figure 8.11c) and often exhibit mutual grain boundaries. Sphalerite commonly contains crystallographically oriented blebs and rods of
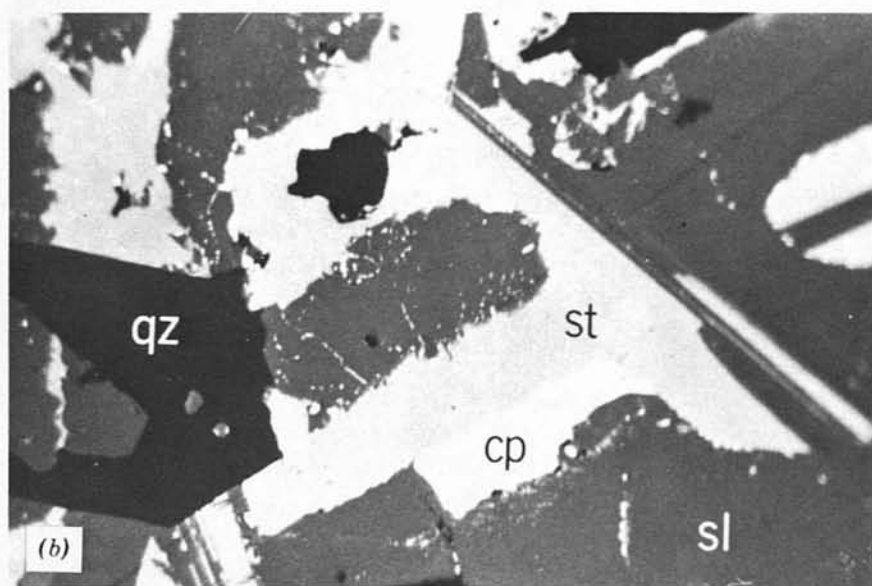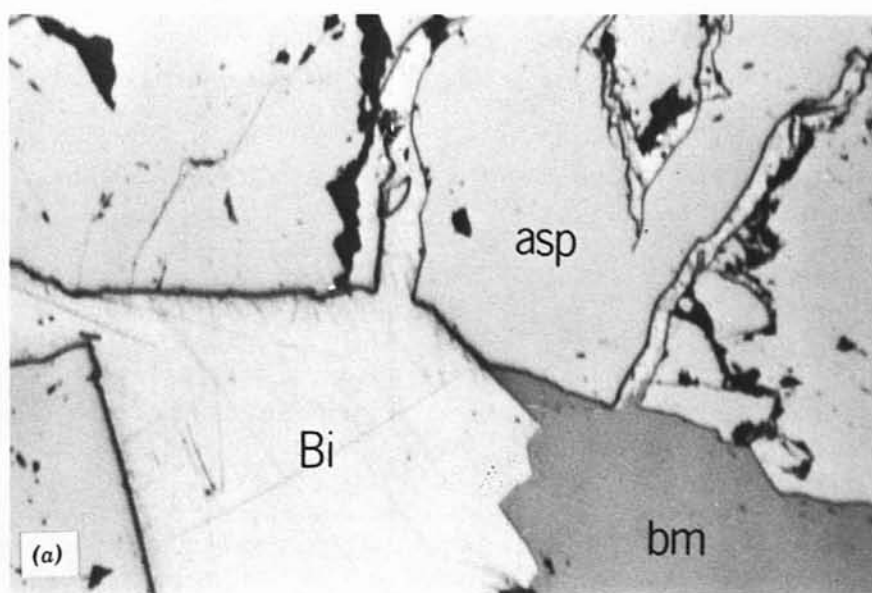
FIGURE 9.23 Ore mineral assemblages in the tin-tungsten ores of Bolivia. (*a*) Veinlets and interstitial areas of bismuthinite (bm) and native bismuth (Bi) in arsenopyrite (asp), Chacaltaya Mine (oil immersion, width of field = 900 μm). (*b*) Crystallographic intergrowth of sphalerite (sl), stannite (st), and chalcopyrite (cp) probably resulting from exsolution. Chalcopyrite, the latest phase to exsolve, has collected along sphalerite-stannite contacts; corroded quartz (qz) crystals also present. Sayaquira District (oil immersion, width of field = 850 μm). (Reproduced from W. C. Kelly and F. S. Turneaure, *Econ. Geol.* **65**, 1970, with permission of the authors and the publisher.)

chalcopyrite, pyrrhotite, and stannite (Figure 9.23b). Chalcopyrite is also present as anhedral polycrystalline masses with pyrrhotite. Franckeite, if present, occurs as plates and blades. The pyrrhotite is often altered along fractures and grain boundaries to pyrite and marcasite (Figure 8.11d). These minerals may also be present as concentric "birds-eye" textures (see Figure 7.35) and boxwork structures. Pyrite may also be present as isolated euhedral or subhedral polycrystalline aggregates. Stannite may be present as anhedral grains (see Figure 8.11b) but most commonly shows an affinity for sphalerite in which it frequently occurs as crystallographically oriented intergrowths (see Figure 8.11d).

9.8.2 Origin of the Ores

Tin-tungsten-bismuth ores have generally been considered to be of magmatic-hydrothermal origin and related to intermediate to acid batholiths and stocks. The veins have formed by sequential open-space deposition of sulfides, oxides, and gangue minerals from brines that were initially NaCl-rich (up to 46 wt %) but that were more dilute in later stages. In the Bolivian tin province, the depositional temperatures in the early stages were $\sim 300°C$ and rose to $530°C$; in the base-metal stage, temperatures ranged from $400–260°C$; during pyrrhotite alteration, the temperature dropped to $260–200°C$. Late veinlets and crustifications formed at temperatures from $200–70°C$ (Kelly and Turneaure, 1970; Turneaure, 1971). Deposition took place at depths between 350 m and 4,000 m at pressures between 30 and 1,000 bars. Fluid inclusion studies indicate that active boiling occurred during early stages of ore deposition and that the vapor transported some mineral matter. The Sn-rich fluids are probably generated during the late stages of fractional crystallization of a granitoid magma (see Groves and McCarthy, 1978).

Sillitoe, Halls, and Grant (1975) have suggested that several of the well-known Bolivian tin deposits should be designated as *porphyry tin deposits.* These authors note that such deposits are similar to porphyry copper deposits (see Section 9.5) in being associated with passively emplaced and pervasively sericite-altered stocks, in having crudely concentric zoning, in containing mineralized breccias, and in containing large volumes of rock with low-grade ores (0.2–0.3% sln). They propose that porphyry tin deposits represent the lower portions of stratovolcanoes.

9.9 GOLD VEIN AND RELATED MINERALIZATION

Mineralogy Economically important ore minerals may include native gold (commonly called "electrum" if it contains 20% or more silver) and precious metal tellurides (e.g., sylvanite, petzite $AuAg_3Te_2$, hessite Ag_2Te, calaverite $AuTe_2$, krennerite $AuTe_2$); associated uneconomic ore minerals may include pyrite, marcasite, arsenopyrite, pyrrhotite in major amounts, and minor

amounts of galena, sphalerite, chalcopyrite, stibnite, tetrahedrite-tennantite, realgar; gangue minerals are dominated by quartz with minor local carbonates (calcite, siderite, ankerite, dolomite), feldspars, tourmaline, fluorite, barite, epidote, and graphite, amorphous carbon, or carbonaceous matter.

Mode of Occurrence   Gold occurs in a wide variety of settings, ranging from volcanic sinters and breccias to porphyrys, skarns, and hydrothermal veins that may or may not be directly associated with intrusions and from dissemination in massive sulfides to placer and palaeoplacer deposits. Veins dominated by native gold and quartz occur in ancient highly deformed and metamorphosed volcanic rocks (notably Precambrian greenstone belts). Veins dominated by gold and silver tellurides with quartz occur in this setting and in young (Tertiary) volcanic rocks of the circum-Pacific belt. In the brief account given here, it is not the intention to discuss the form, setting, and origin of the many diverse types of gold occurrence, but rather, to outline briefly the (generally rather similar) ore mineralogy. General accounts of the geochemistry of gold have been presented by Boyle (1979) and Romberger (1989), and the nature of gold occurrences worldwide has been summarized by Boyle (1979).

Examples   Gold-quartz vein mineralization includes deposits at Yellowknife (N.W.T., Canada), the Mother Lode (California, United States), and the Homestake Mine (S. Dakota, United States); gold and silver tellurides occur in Precambrian rocks at Kalgoorlie (W. Australia), Kirkland Lake and Porcupine (Canada); gold and silver tellurides occur in Tertiary volcanics in Fiji, the Phillipines, Japan, and California-Colorado-Nevada-New Mexico (United States). Placer gold deposits include examples in California, Alaska, United States; the Urals, Russia; Otago area, New Zealand.

9.9.1   Mineral Associations and Textures

As is typical of fissure-filling veins, many show crustification and the development of well-formed quartz and carbonate crystals, although movement along the fractures can destroy many of these textures, leaving a granular ore. The gold in the gold-quartz veins occurs within quartz or within, or marginal to, pyrite or arsenopyrite and is generally very fine-grained (Figure 9.24). In the veins that contain gold-silver tellurides, these occur as small irregular masses within quartz and are often a complex intergrowth of many minerals, including, in addition to those listed already, a variety of other telluride minerals, native tellurium, and various sulfides and sulfosalts, all in very minor amounts. The mineral assemblages and the paragenetic sequences are complex, but generalizations can sometimes be made. For example, the ores of Boulder County, Colorado, studied in detail by Kelly and Goddard (1969), show a generalized paragenesis in which early quartz and fluorite are succeeded by sulfides, tellurides, native gold and then by carbonates and quartz.
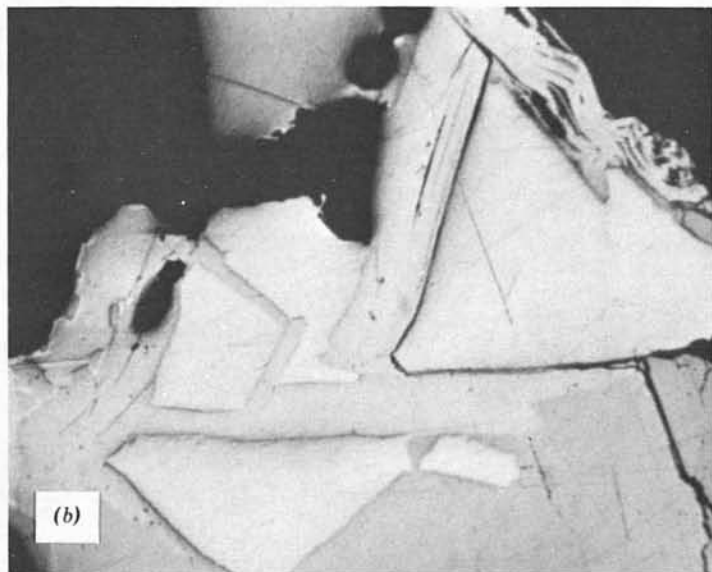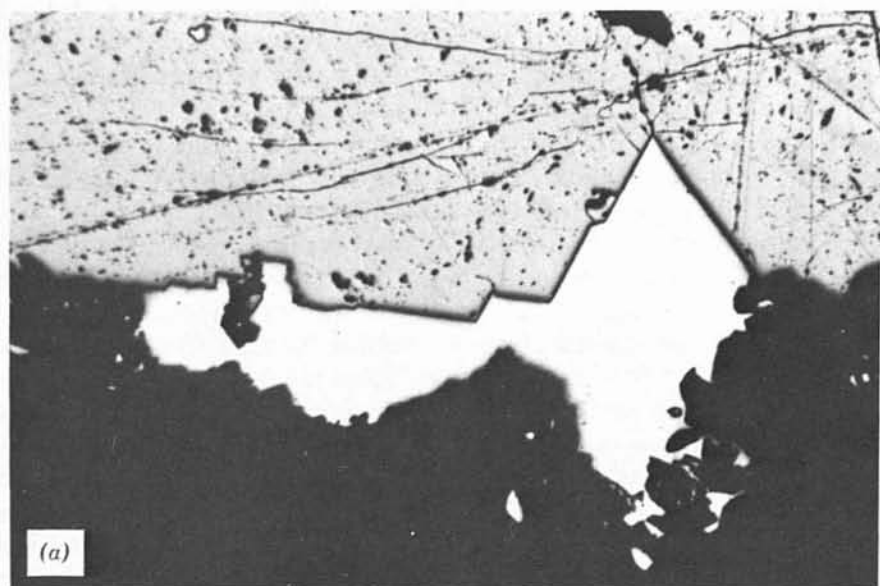
FIGURE 9.24 Typical occurrences of gold in vein and related ores. (*a*) Gold bordering arsenopyrite, Homestake Mine, South Dakota (width of field = 2,000 µm). (*b*) Angular gold grains with galena (darker gray) and tetradymite (light gray adjacent to gold) in a quartz vein deposit, Mineral Ridge, Fairfax Co., Virginia, (width of field = 2,000 µm).

Fluid inclusion studies indicate that hydrothermal solutions with salinites of 20–30% precipitated the early quartz and fluorite between 250°C and 375°C. Gold deposition occurred from solutions with only about 4% salinity at 205–270°C (Nash and Cunningham, 1973).

Boyle (1979) has summarized the geothermometric studies that have been carried out on epigenetic gold deposits and has concluded that the bulk of quartz and sulfide mineralization took place between 500°C and 150°C, with much gold having been redistributed at lower temperatures. He has given a further detailed discussion of the paragenesis and zoning of epigenetic gold deposits.

The interpretation of assemblages and textures of the gold-silver tellurides has been clarified by studies of the phase relations in the Au-Ag-Te system. Markham (1960) and Cabri (1965) have presented the phase relations at 300°C and 290°C, respectively, as shown in Figure 9.25; the differences between these diagrams probably reflect the rapid quench techniques of Cabri, whose results may be closer to the true relations at 290°C. The results of Markham may reflect some readjustment of compositions to lower temperatures and may more closely approximate final products of cooling in the natural ores. Comparison of synthetic and natural assemblages indicates that melting phe-
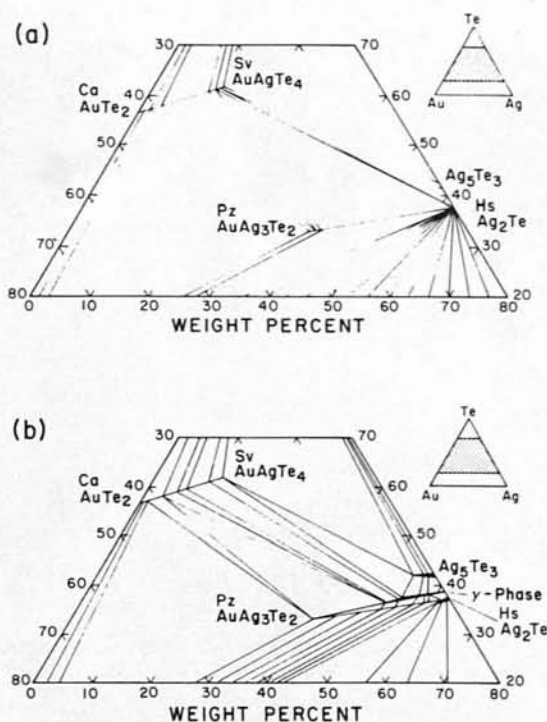

FIGURE 9.25 Phase relations in the central portion of the Au-Ag-Te system: (*a*) at 300°C (after Markham, 1960); (*b*) at 290°C (after Cabri, 1965).

nomena or telluride melts (which can occur at temperatures as low as 304°C) have played no significant role in producing the observed assemblages, most of which have resulted from subsolidus processes and equilibrated at relatively low temperatures (below ~250°C).

9.9.2 Origin of the Ores

There is little doubt that these ores have formed by deposition from hydrothermal solutions into open fissure and fracture systems. The absence of parent intrusions and extensive hydrothermal alteration has led Worthington and Kiff (1970) to suggest that many gold deposits formed during the waning stages of volcanism. In the case of the gold-quartz veins in highly deformed and metamorphosed volcanics and sediments, it is widely thought that the gold may have been derived from the enclosing rocks and may have been concentrated by circulating fluids during metamorphism. The feasibility of such mechanisms has been discussed by Fyfe and Henley (1973). The Tertiary deposits clearly indicate a volcanic source for the ore-bearing hydrothermal solutions, although, in the case of those telluride gold deposits in older rocks, the role of volcanic or intrusive igneous rocks as sources for the hydrothermal fluids is much less certain. The compositions of these hydrothermal fluids and whether the gold is transported as gold-sulfur or gold-chloride complexes are also matters of debate (Fyfe and Henley, 1973).

9.10 ARSENIC-, ANTIMONY-, OR MERCURY-BEARING BASE-METAL VEIN DEPOSITS

This broad category includes ores rich in copper-zinc but having significant amounts of arsenic (Butte, Montana), lead-zinc-silver ores rich in antimony and arsenic (Coeur d'Alene, Idaho), arsenic-antimony ores (Getchell, Nevada), and mercury sulfide ores (Almaden, Spain). The diversity of these ores requires individual mineral summaries.

Mode of Occurrence The ores included in this section occur as massive to disseminated infillings in faults and fractures and as replacement bodies often in close proximity to acid or intermediate intrusions. Zoning of copper, zinc, arsenic, and sulfur is common both laterally and vertically in the vein systems. Wall rock alteration in the form of feldspathization, sericitization, argillization, and bleaching is frequently developed adjacent to the sulfide ores.

9.10.1 Copper-Zinc-Arsenic

Mineralogy
Major   Pyrite, chalcopyrite, bornite, tennantite,
                             sphalerite, enargite

Minor   Covellite, hematite, magnetite, chalcocite,
                               digenite, galena, molybdenite
Gangue Minerals   Quartz, siderite, calcite, barite, rhodochrosite.

Examples Butte, Montana; Magma Mine, Arizona; Tsumeb, South Africa;
Bor, Yugoslavia.

9.10.2 Mineral Associations and Textures

On the macroscopic scale, these ores, as do other vein ores, often display a distinct zoning parallel to the axis of the vein; more or less well-defined bands rich in pyrite, chalcocite, covellite, bornite, enargite, and so on, occur discontinuously with widths varying from millimeters to meters. Grain size is highly variable but is frequently 0.5 mm to 1 cm or more; hence, individual minerals are readily recognized with the naked eye. Microscopically, it is apparent that many of the large grains lie in a matrix of, or are themselves composed of, intimate irregular fine-grained intergrowths of bornite, chalcocite, chalcopyrite, bornite, enargite, and copper sulfides (covellite, digenite, djurleite). Common lath-like and "basket weave" textures in the copper sulfides and between chalcopyrite and bornite reflect exsolution from solid solutions at the higher temperatures of ore formation. As is evident from Figure 10.8, a single-phase chalcocite-digenite solid solution that forms at an elevated temperature can decompose to form a mixture of low-temperature copper sulfides on cooling. The resulting texture is commonly one of intersecting laths. Spectacular covellite-rich portions of these ores consist of coarse but highly fractured aggregates that are crisscrossed with fine veinlets of later covellite or other copper sulfides (Figure 9.26a). Pyrite is abundant in these ores, often occurring repeatedly in the paragenesis; early-formed pyrite is commonly deeply corroded and replaced by chalcopyrite, bornite, enargite, and other phases (Figure 9.26b).

High-temperature relationships between the copper-iron sulfides are well characterized, but this is not true of the stable low-temperature associations (Figure 8.17b). The frequent association of pyrite and bornite as seen in these ores was long thought to be indicative of formation above 228°C (Yund and Kullerud, 1966), but it now appears that this association reflects stable lower-temperature relationships.

Sphalerite is a major but erratically distributed mineral occurring as disseminated grains, veinlets, and coarsely crystalline masses. Oriented rows of chalcopyrite blebs (so-called chalcopyrite disease) are common in the sphalerite. Tennantite series minerals are also irregular in distribution and are present as scattered irregular blebs and patches, as veinlets, and as pods up to meters across. Except in the pods where large (>1 cm) grains occur, the tennantite is intimately intergrown with bornite, chalcocite, and enargite. Hematite is locally abundant as randomly oriented clusters of radiating laths interspersed with pyrite, bornite, chalcopyrite, and enargite.
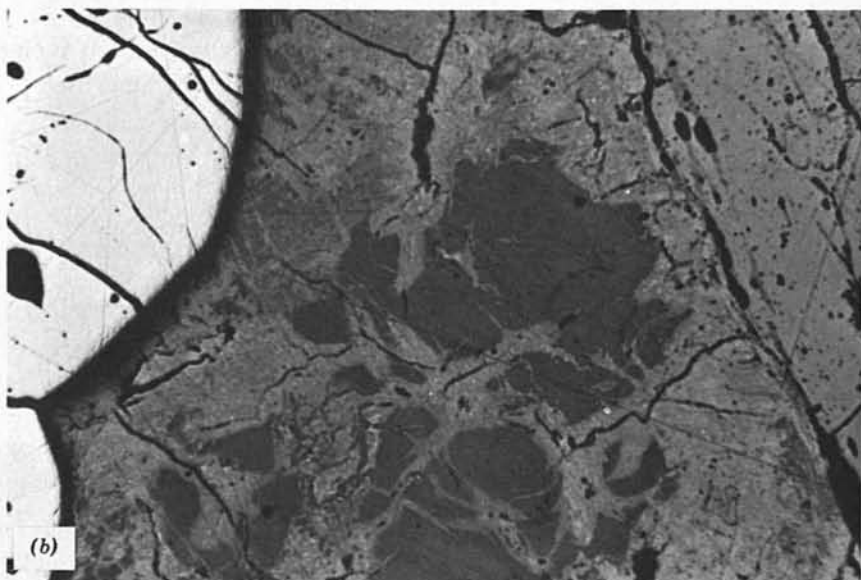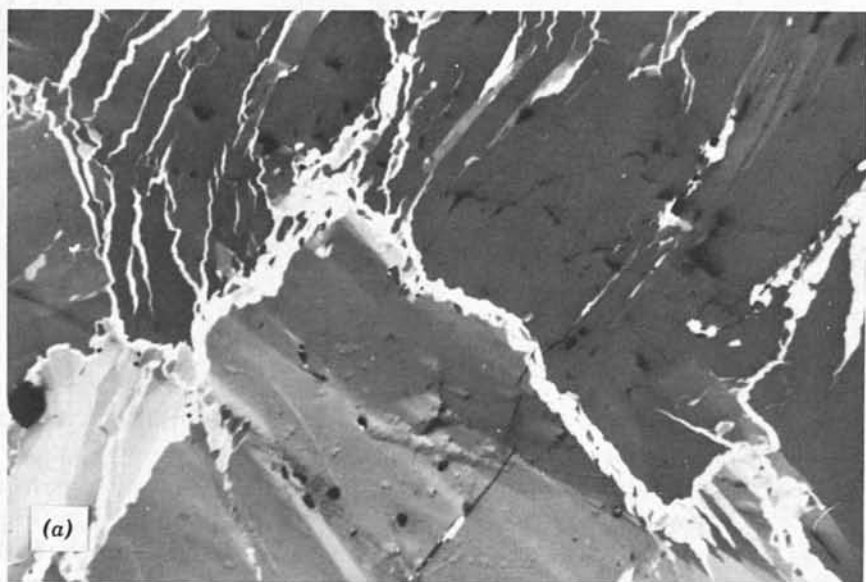
FIGURE 9.26 Typical ores of copper-zinc-arsenic affiliation. (*a*) Coarse aggregate of covellite (gray) veined by later chalcocite, Butte, Montana (width of field = 2,000 μm). (*b*) Islands of bornite in chalcocite flanked by enargite (on right) and pyrite (white), Butte, Montana (width of field = 2,000 μm).

9.10.3   Lead-Zinc-Silver Ores with Antimony and Arsenic

Mineralogy

Major	Galena, sphalerite, tetrahedrite, chalcopyrite
Minor	Pyrite, pyrrhotite, arsenopyrite, magnetite
Gangue Minerals	Quartz, siderite, dolomite, barite

Examples   Coeur d'Alene District, Idaho; Kapnik, Czechoslovakia; Andreasberg, Germany; Freiberg, Saxony.

9.10.4   Mineral Associations and Textures

These ores occur as compact, generally fine-grained vein fillings with major mineral dominance varying from one part of a district or vein to another. All ore minerals, with the exception of locally disseminated and often corroded pyrite cubes, are anhedral, with grain sizes usually less than 0.5 mm (Figure 9.27a). Galena may contain small amounts of accessory metals, but the bulk of the silver is present in tetrahedrite, which is abundant as small rounded islands dispersed throughout (Figure 9.27b). In tetrahedrite-rich portions of the ore, the galena occurs as small cusp-like grains. Chalcopyrite is present as small anhedral grains and irregular veinlets. Sphalerite, dispersed as grains and veinlets, is generally light in color and contains relatively little (usually less than 5%) iron and small amounts of manganese and cadmium. Occasionally, the sphalerite contains oriented rows of chalcopyrite inclusions.

The well-known Coeur d'Alene ores have been metamorphosed such that shearing, brecciation, and curved cleavages in galena are abundant.

### 9.10.5   Arsenic-Antimony Sulfide Ores

Mineralogy

|	
Major	Realgar, orpiment, pyrite, stibnite
Minor	Chalcopyrite, arsenopyrite, gold, marcasite
Gangue Minerals	Quartz, calcite, carbon, sericite, chlorite

Examples   Getchell, Nevada; Elbrus, Caucasus; Uj-Moldava, Romania.

9.10.6   Mineral Associations and Textures

These unique and colorful ores consist of intergrown coarse-grained (>0.1 mm) aggregates varying from realgar-rich to orpiment-rich. Overgrowth, interpenetration, and replacement of one As-sulfide by another is common and leaves an overall chaotic texture. Pyrite, when present, occurs as subhedral to euhedral grains that are either isolated or in irregular thin veinlets. Stibnite occurs locally as fine, commonly radiating laths dispersed within the As-sulfides.
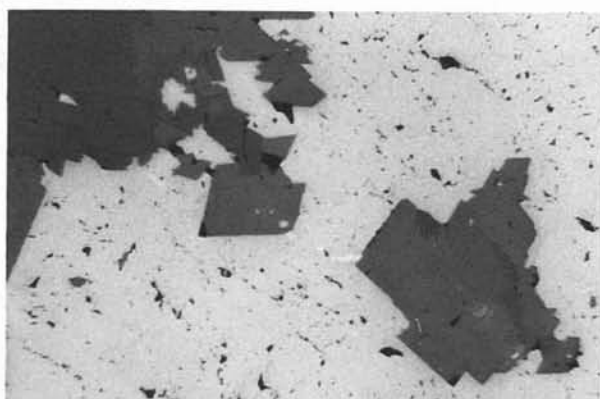
(a)
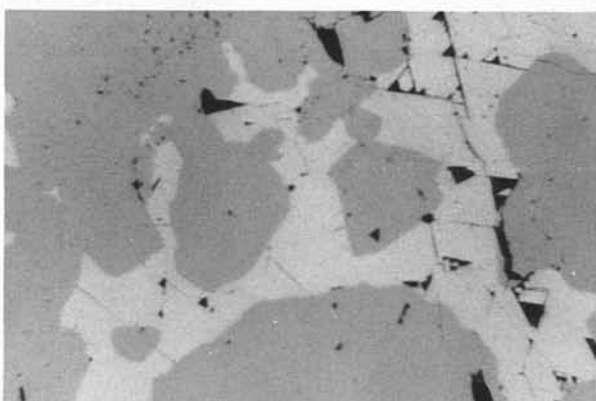
(b)

FIGURE 9.27 Lead-zinc-silver ores with antimony and arsenic from the Coeur d'Alene District, Idaho. (*a*) Tetrahedrite with traces of chalcopyrite; the characteristic rhombs of siderite ($FeCO_3$) are clearly visible. (*b*) Intergrown tetrahedrite (darker gray) and galena (note cleavages in the galena only), Bunker Crescent Mine (width of field = 1,200 μm).

9.10.7 Mercury Sulfide Vein Deposits

Mineralogy

Major	Cinnabar, metacinnabar, pyrite, marcasite
Minor	Native mercury, stibnite, sphalerite, pyrrhotite
Gangue Minerals	Quartz, chalcedony, barite, dolomite, clay minerals

Examples   Almaden, Spain; Idria, Trsce, Yugoslavia; Sulphur Bank, Amedee Hot Springs, New Idria, New Almaden, California; Steamboat Springs, Cordero, Nevada; Amiata, Italy; Huancavalica, Peru.
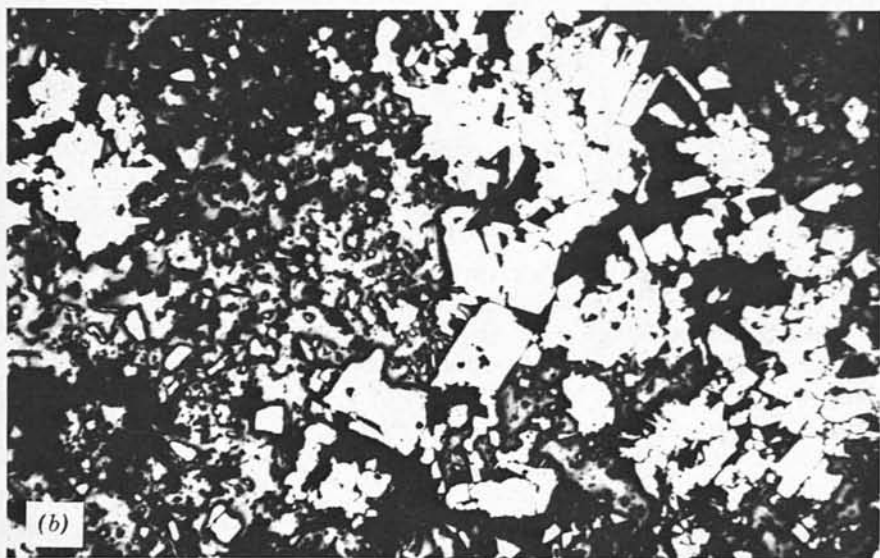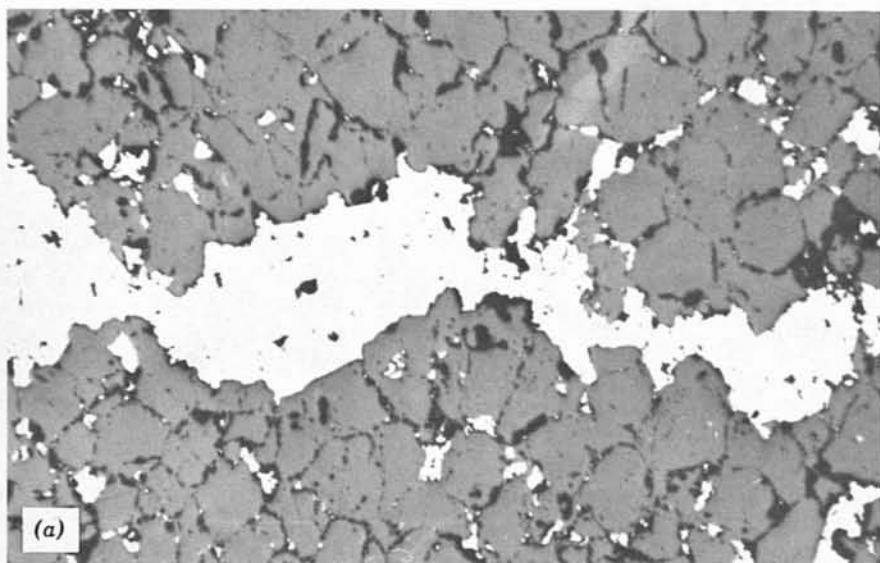
FIGURE 9.28 Mercury sulfide ores. (*a*) Veinlet of cinnabar in quartzite, Almadén, Spain (width of field = 2,000 μm). (*b*) Subhedral crystals of pyrite and marcasite within a matrix of cinnabar, New Idria, California (width of field = 2,000 μm).

9.10.8 Mineral Associations and Textures

Cinnabar and, locally, metacinnabar occur in these ores as fine-grained (0.1–1 mm) euhedral single crystals, small polycrystalline aggregates (up to 5 mm), and as stringers, veinlets, and intergranular cements (Figure 9.28a). In some

areas, cinnabar occurs in alternating veinlets with dolomite and quartz. Pyrite and marcasite occur with the mercury sulfides as isolated subhedral to euhedral crystals and polycrystalline veinlets (Figure 9.28b). Stibnite occurs locally as very fine (< 0.1 mm) acicular crystals. Native mercury also appears locally. It may appear from within samples when they are broken, cut, or even cast. Mercury vapors should be avoided, and it is, of course, impossible to polish liquid mercury containing samples.

Cinnabar, frequently possessing minor amounts of metacinnabar and stibnite, is well known as grain coatings and vug fillings in tufa and sinter deposits associated with hot-spring activity (Dickson and Tunell, 1968; Weissberg, Browne, and Seward, 1979). The mercury sulfides form wispy polycrystalline layers of crystals (usually less than 100 mm across) within, or on which, stibnite grows as individual acicular crystals and rosette-like clusters.

REFERENCES

Badham, J. P. N., Robinson, B. W., and Morton, R. D. (1972). The geology and genesis of the Great Bear Lake Silver Deposits. 24th Int. Geol. Cong. (Montreal), Section 4, 541–548.

Barnes, H. L. (1979). Solubilities of Ore Minerals. In H. L. Barnes (ed.), *Geochemistry of Hydrothermal Ore Deposits*, 2nd ed. Wiley-Interscience, New York, pp. 401–460.

Bateman, A. M. (1951). The formation of late magmatic oxide ores. *Econ. Geol.* **46**, 404–426.

Boyle, R. A. (1979). The geochemistry of gold and its deposits. *Can. Geol. Surv. Bull.* **280**.

Buddington, A. F., and D. H. Lindsley (1964). Iron-titanium oxide minerals and synthetic equivalents. *J. Petrol.* **5**, 310–357.

Cabri, L. J. (1965). Phase relations in the system Au-Ag-Te and their mineralogical significance. *Econ. Geol.* **60**, 1569–1606.

Campbell, I. H., Naldrett, A. J., and Barnes, S. J. (1983). A model for the origin of platinum-rich sulfide horizons in the Bushveld and Stillwater Complexes. *Jour. of Petrology* **24**, 133–165.

Cox, D. P., and Singer, D. A. (1986). Mineral deposit models. *U.S. Geol. Survey Bulletin* 1963, 393 pp.

Dickey, J. S., Jr. (1975). A hypothesis of origin of podiform chromite deposits. *Geochim. Cosmochim. Acta* **39**, 1061–1074.

Dickson, F. W., and Tunell, G. (1968). Mercury and antimony deposits associated with active hot springs in the western United States. In J. D. Ridge (ed.), *Ore Deposits in the United States, 1933–1967*, Vol. 2. A.I.M.E., New York, pp. 1673–1701.

Fyfe, W. S., and Henley, R. W. (1973). Some thoughts on chemical transport processes with particular reference to gold. *Mineral. Sci. Eng.* **5**, 295–303.

Groves, D. I., and McCarthy, T. S. (1978). Fractional crystallization and the origin of tin deposits in granitoids. *Mineral. Deposita* **13**, 11–26.

Hall, W. E., Friedman, I., and Nash, J. T. (1974). Fluid inclusion and light stable isotope study of the Climax molybdenum deposits, Colorado. *Econ. Geol.* **69**, 884–911.

Halls, C., and Stumpfl, E. F. (1972). The five elements (Ag-Bi-Co-Ni-As)—a critical appraisal of the geological environments in which it occurs and of the theories affecting its origin. 24th Int. Geol. Cong. (Montreal), Section 4, 540.

Irvine, T. N. (1974). Crystallization sequences in the Muskox Intrusion and other layered intrusions II. Origin of chromitite layers and similar deposits of other magmatic ores. *Geochim. Cosmochim. Acta* **39**, 991–1020.

———. (1977). Origin of chromitite layers in the Muskox and other stratiform intrusions: a new interpretation. *Geology* **5**, 273–277.

Jambor, J. L. (1971). "Origin of the silver veins." In The silver-arsenide deposits of the Cobalt-Gowganda region, Ontario. *Can. Mineral.* **11**, 402–412.

Kelly, W. C., and Goddard, E. N. (1969). Telluride ores of Boulder County, Colorado. *Geol. Soc. Am. Mem.* **109**.

Kelly, W. C., and Turneaure, F. S. (1970). Mineralogy, paragenesis and geothermometry of the tin and tungsten deposits of the Eastern Andes, Bolivia. *Econ. Geol.* **65**, 609–680.

Lago, B. L., Rabinowicz, M., and Nicholas, A. (1982). Podiform chromite ore bodies: a genetic model. *Jour. of Petrology* **23**, 103–125.

Lindsley, D. H. (1991). Oxide Minerals: Petrologic and Magnetic Significance. Revs. in *Mineral* **25**, Min. Soc. America.

Lowell, J. D. (1974). Regional characteristics of porphyry copper deposits of the Southwest. *Econ. Geol.* **69**, 601–617.

Lowell, J. D., and Guilbert, J. M. (1970). Lateral and vertical alteration mineralization zoning in porphyry ore deposits. *Econ. Geol.* **65**, 373–408.

Markham, N. L. (1960). Synthetic and natural phases in the system Au-Ag-Te (Part 1). *Econ. Geol.* **55**, 1148–1178.

Meyer, C., and Hemley, J. J. (1967). Wall rock alteration. In H. L. Barnes (ed.), *Geochemistry of Hydrothermal Ore Deposits.* Holt, Rinehart and Winston, New York, pp. 166–235.

Mitchell, A. H. G., and Garson, M. S. (1972). Relationship of porphyry coppers and circum-Pacific tin deposits to palaeo-Benioff zones. *Min. Metall.* **81**, B10–B25.

Moore, W. J., and Nash, J. T. (1974). Alteration and fluid inclusion studies of the porphyry copper ore body at Bingham, Utah. *Econ. Geol.* **69**, 631–645.

Nash, J. J., and Cunningham, C. G. (1973). Fluid inclusion studies of the fluorspar and gold deposits, Jamestown District, Colorado. *Econ. Geol.* **68**, 1247–1262.

Paktunc, A. D. (1990). Original of Podiform chromite deposits by multistage melting, melt segregation and magma mixing in the upper mantile. *Ore Geology Reviews* **5**, 211–222.

Petruk, W. (1968). Mineralogy and origin of the Silverfields silver deposit in the Cobalt area, Ontario. *Econ. Geol.* **63**, 512–531.

———. "Mineralogical characteristics of the deposits and textures of the ore minerals." In The silver-arsenide deposits of the Cobalt-Gowganda region, Ontario. *Can. Mineral.* **11**, 108–139.

———. "Depositional history of the ore minerals." In The silver-arsenide deposits of the Cobalt-Gowganda region, Ontario. *Can. Mineral.* **11**, 369–401.

Philpotts, A. R. (1967). Origin of certain iron-titanium oxide and apatite rocks. *Econ. Geol.* **62**, 303–330.

Roedder, E. (1971). Fluid inclusion studies on the porphyry type ore deposits at Bingham, Utah; Butte, Montana; and Climax, Colorado. *Econ. Geol.* **66**, 98–120.

Roedder, E. (1977). Fluid inclusions as tools in mineral exploration. *Econ. Geol.* **72**, 503–525.

———. (1979). Fluid inclusions as samples of ore fluids. In H. L. Barnes (ed.), *Geochemistry of Hydrdothermal Ore Deposits*, 2nd ed., Wiley-Interscience, New York, pp. 684–737.

Romberger, S. B. (1989). Geochemistry of gold in hydrothermal deposits. In D. R. Shawe and R. P. Ashley (eds.), Geology and resources of gold in the United States. *U.S. Geol. Survey Bull.*, No. 1857A, 9–25.

Rose, A. W., and Burt, D. M. (1979). Hydrothermal alteration. In H. L. Barnes (ed.), *Geochemistry of Hydrothermal Ore Deposits*, 2nd ed., Wiley-Interscience, New York, pp. 173–235.

Rumble, D., ed. (1976). Oxide minerals. Mineral. Soc. Am. Short Course Notes, Vol. 3 (a collection of papers, several of which deal with iron-titanium oxides).

Scott, S. D. (1972). The Ag-Co-Ni-As ores of the Siscoe Metals of Ontario Mine, Gowganda, Ontario, Canada. 24th Int. Geol. Cong., Section 4, 528–538.

Scott, S. D., and O'Connor, T. P. (1971). "Fluid inclusions in vein quartz, Silverfields Mine, Cobalt, Ontario." In The silver-arsenide deposits of the Cobalt-Gowganda region, Ontario. *Can. Mineral.* **11**, 263–271.

Sillitoe, R. H. (1972). A plate tectonic model for the origin of porphyry copper deposits. *Econ. Geol.* **67**, 184–197.

———. (1973). The tops and bottoms of porphyry copper deposits. *Econ. Geol.* **68**, 799–815.

Sillitoe, R. H., Halls, C., and Grant, J. N. (1975). Porphyry tin deposits in Bolivia. *Econ. Geol.* 913–927.

Turneaure, F. S. (1971). The Bolivian tin-silver province. *Econ. Geol.* **66**, 215–225.

Weissburg, B. G., Browne, P. R. L., and Seward, T. M. (1979). Ore metals in active geothermal systems. In H. L. Barnes (ed.), *Geochemistry of Hydrothermal Ore Deposits*, 2nd ed., Wiley-Interscience, New York, pp. 738–780.

Worthington, J. E., and Kiff, I. T. (1970). A suggested volcanogenic origin for certain gold deposits in the slate belt of the North Carolina Piedmont. *Econ. Geol.* **65**, 529–537.

Yund, R. A., and G. Kullerud (1966). Thermal stability of assemblages in the Cu-Fe-S system. *J. Petrol.* **7**, 454–488.

BIBLIOBRAPHY

Burnham, C. W. (1979). Magmas and Hydrothermal Fluids. In H. L. Barnes (ed.), *Geochemistry of Hydrothermal Ore Deposits*, 2nd ed. John Wiley and Sons, New York, pp. 71–136.

Canadian Mineralogist (1979). Nickel-sulfide and platinum-group-element deposits. **17**: 2 (1979), 141–514.

Duke, J. M. (1983). Ore deposit models F. Magmatic segregation deposits of chromite. *Geoscience Canada* **10**, 15–24.

Economic Geology (1976). An issue devoted to platinum-group elements. **71**: 7, 1129–1468.

Economic Geology (1978). The Number 5 issue is devoted to "Porphyry Copper Deposits of the Southwestern Pacific Islands and Australia."

Economic Geology (1978). The Number 7 issue is devoted to "The Bingham Mining District."

Economic Geology (1981). A special issue on nickel deposits and their host rocks in Western Australia. V. 76, no. 6.

Economic Geology (1984). A second issue devoted to Canadian mineral deposits. V. 79, no. 5.

Economic Geology (1984). A special issue on massive sulfide deposits of the Appalachian-Caledonian Orogen. V. 79, no. 7.

Economic Geology (1985). A special issue devoted to the Bushveld Complex. V. 80, no. 4.

Economic Geology (1988). A special issue devoted to the geology and mineral deposits of Mexico. V. 83, no. 8.

Economic Geology (1989). A special issue devoted to current research on mineral deposits of Europe. V. 84, no. 5.

Economic Geology (1990). A special issue devoted to the mineral deposits of Peru. V. 85, no. 7.

Economic Geology (1992). A special issue devoted to Australian volcanic-hosted massive sulfide (VHMS) deposits and their volcanic environment. V. 87, no. 3.

Economic Geology (1993). A special issue devoted to Abitibi ore deposits in a modern context. V. 88, no. 6.

Ewers, W. E., and Hudson, D. R. (1972). An interpretive study of a nickel-iron sulfide ore intersection, Lunnon Shoot, Kambalda, Western Australia. *Econ. Geol.* **67**, 1075–1092.

Foley, N. K., Bethke, P. M., and Rye, R. O. (1989). A reinterpretation of the δDH_2O of inclusion fluids in contemporaneous quartz and sphalerite, Creede Mining District, Colorado: A genetic problem for shallow ore bodies? *Econ. Geol.* **84**, 1966–1977.

Force, E. R. (1991). Geology of titanium-mineral deposits. *Geol. Soc. Amer. Spec. Paper* **259**, 112 pp.

Fryklund, V. C. (1964). Ore deposits of the Coeur d'Alene District, Shoshone County, Idaho. U.S. Geol. Surv. Prof. Paper No. 445.

Hammer, D. F., and Peterson, D. W. (1968). Geology of the Magma Mine area, Arizona. In J. D. Ridge (ed.), *Ore Deposits in the United States, 1933–1967*, Vol. 2. A.I.M.E., New York, pp. 1282–1310.

Hawley, J. E. (1962). The Sudbury ores: their mineralogy and origin. *Can. Mineral.* **7**, 1–207.

Helgeson, H. C. (1970). A chemical and thermodynamic model of ore deposition in hydrothermal systems. *Min. Soc. Am.* Special Paper **3**, 155–186.

———. (1979). Mass transport among minerals and hydrothermal solutions. In H. L. Barnes (ed.), *Geochemistry of Hydrothermal Ore Deposits*, 2nd ed. Wiley-Interscience, New York, pp. 568–610.

Keays, R. R., Ramsay, W. R. H., and Groves, D. I. (1989). The geology of gold deposits: the perspective in 1988. *Econ. Geol. Monograph* **6**, 667 pp.

Kelly, D. P., and Vaughan, D. J. (1983). Pyrrhotite-pentlandite ore textures: a mechanistic approach. *Mineral Magazine* **47**, 453–463.

Kelly, W. C., and Rye, R. O. (1979). Geologic, fluid inclusion, and stable isotope studies of the tin-tungsten deposits of Panasqueira, Portugal. *Econ. Geol.* **74**, 1721–1822.

Kettaneh, Y. A., and Badham, J. P. N. (1978). Mineralization and paragenesis at the Mount Wellington Mine, Cornwall. *Econ. Geol.* **43**, 486–495.

Koschmann, A. H., and Bergendahl, M. H. (1968). Principal gold-producing districts of the United States. U.S. Geol. Surv. Prof. Paper 610.

Linn, R. K. (1968). New Idria Mining District. In J. D. Ridge (ed.), *Ore Deposits in the United States, 1933-1967*, Vol. 2. A.I.M.E., New York, pp. 1623–1649.

Lister, G. F. (1966). The composition and origin of selected iron-titanium deposits. *Econ. Geol.* **61**, 275–310.

Macdonald, A. J. (1987). Ore deposit models #12: the platinum group element deposits: classification and genesis. *Geoscience Canada* **14**, 155–166.

McMillan, W. J., and Panteleyer, A. (1980). Ore deposit models—1 porphyry copper deposits. *Geosci. Canada* **7**, 52–63.

Meyers, C., et al. (1968). Ore deposits at Butte, Montana. In J. D. Ridge (ed.), *Ore Deposits in the United States, 1933-1967*, Vol. 2. A.I.M.E., New York, pp. 1374–1416.

Morris, H. T., Fisher, F. S., Shawe, D. R., and Thompson, T. B. (1990). Gold-bearing polymetallic veins and replacement deposits—Part II. U.S. Geol. Surv. Bull, No. 1857-F, 49 pp.

Naldrett, A. J. (1989). Magmatic sulfide deposits. *Oxford Monographs on Geology and Geophysics* Vol. 14, Oxford University Press, 186 pp.

Naldrett, A. J., Craig, J. R., and Kullerud, G. (1967). The central portion of the Fe-Ni-S system and its bearing on pentlandite exsolution in iron-nickel sulfide ores. *Econ. Geol.* **62**, 826–847.

Nash, T. J. (1975). Geochemical studies in the Park City District: II. Sulfide mineralogy and minor-element chemistry, Mayflower Mine. *Econ. Geol.* **70**, 1038–1049.

Ohmoto, H. (1972). Systematics of sulfur and carbon isotopes in hydrothermal ore deposits. *Econ. Geol.* **67**, 551–578.

Ohmoto, H., and Rye, R. O. (1970). The Bluebell Mine, British Columbia. I. Mineralogy, paragenesis, fluid inclusions and the isotopes of hydrogen, oxygen and carbon. *Econ. Geol.* **65**, 417–437.

Polya, D. A. (1989). Chemistry of the Mainstage ore-forming fluids of the Panasqueira W-Cu(Ag)-Sn deposit, Portugal: implications for models of ore genesis. *Econ. Geol.* **84**, 1134–1152.

Roedder, E. (1972). Composition of fluid inclusions (Data of Geochemistry Series). U.S. Geol. Survey Prof. Paper 440 JJ.

Saupe, F. (1973). La Géologie du Gisement de Mercure d'Almaden. *Sci. Terre Mem.* **29**.

Sheppard, S. M. F., Nielson, R. L., and Taylor, H. P. (1971). Hydrogen and oxygen isotope ratios in minerals from porphyry copper deposits. *Econ. Geol.* **66**, 515–542.

Skinner, B. J., White, D. E., Rose, H. J., and Mays, R. E. (1967). Sulfides associated with the Salton Sea geothermal brine. *Econ. Geol.* **62**, 316–330.

Slaughter, A. L. (1968). The homestake mine. In J. D. Ridge (ed.), *Ore Deposits in the United States, 1933–1967*, Vol. 2. A.I.M.E., New York, pp. 1436–1459.

Taylor, H. P. (1974). The application of oxygen and hydrogen isotope studies to problems of hydrothermal alteration and ore deposition. *Econ. Geol.* **69**, 843–883.

Tunell, G. (1964). Chemical processes in the formation of mercury ores and ores of mercury and antimony. *Geochim. Cosmochim. Acta* **28**, 1019–1037.

Vaughan, D. J., Schwarz, E. J., and Owens, D. R. (1971). Pyrrhotites from the Strathcona Mine, Sudbury, Canada: a thermomagnetic and mineralogical study. *Econ. Geol.* **66**, 1131–1144.

Wallace, S. R., MacKenzie, W. B., Blair, R. G., and Muncaster, N. K. (1978). Geology of the Urad and Henderson molybdenite deposits, Clear Creek County, Colorado, with a section on a comparison of these deposits with those at Climax, Colorado. *Econ. Geol.* **73**, 325–368.

Wallace, S. R., Muncaster, N. K., Jonson, D. C., MacKenzie, W. B., Bookstrom, A. A., and Surface, V. E. (1968). Multiple intrusion and mineralization at Climax, Colorado. In John D. Ridge (ed.), *Ore Deposits of the United States 1933/1967*, Vol. 1 (Graton-Sales Volume). A.I.M.E., New York, pp. 605–640.

White, D. E. (1967). Mercury and base-metal deposits with associated thermal and mineral waters. In H. L. Barnes (ed.), *Geochemistry of Hydrothermal Ore Deposits*. Holt, Rinehart and Winston, New York, pp. 575–631.

_____. (1968). Environments of generation of some base-metal ore deposits. *Econ. Geol.* **63**, 301–335.

_____. (1974). Diverse origins of hydrothermal ore fluids. *Econ. Geol.* **69**, 954–973.

Wilson, H. D. B., ed. (1969). *Magmatic ore deposits: a symposium. Econ. Geol.* Monograph No. 4.